Nanocomposite immunosensor for anti-transglutaminase antibody

Natasha West

A thesis submitted in fulfillment of the requirements for the degree of Magister Scientiae in the Department of Chemistry, University of Western Cape.

Supervisors: Prof. Emmanuel I. Iwuoha and Prof. Priscilla Baker.

November 2009

KEYWORDS

Biosensor

Immunosensor

Polypyrrole

Gold nanoparticles

Cyclic voltammetry

Square wave voltammetry

Electrochemical impedance spectroscopy

Coeliac disease

Transglutaminase (tTG) antigen

Anti-transglutaminase antibodies

ABSTRACT

Coeliac disease (CD) is a gluten intolerance condition that results in the flattening of the villi, which line the bowel. It is the most common cause of malabsorption of food nutrients. This inability to absorb sufficient levels of nutrients causes many of the common symptoms experienced by CD patients. Some of the symptoms, which lead to an increase in mortality rate, include chronic diarrhea, fatigue, iron-deficient anemia and osteoporosis. People with CD have higher than normal levels of certain antibodies in their blood. Thus, the concentration of anti-transglutaminase antibody (anti-tTG) in human sera is an important analytical marker for the diagnosis of CD. An immunosensor is a type of biosensor that has an antigen or antibody fragment as its biological recognition component. The specificity of the molecular recognition of antigens by antibodies to form a stable complex is the basis of immunosensor technology. In this work, overoxidized polypyrrole (OvoxPpy) was electrosynthesized as a noval sensor platform on a glassy carbon electrode (GCE). The OvoxPpy was then doped with gold-nanoparticles (GNP) by electrodeposition using cyclic voltammetry to form GNP|OvoxPpy||GCE electrode system. Morphology and size of the GNP|OvoxPpy||GCE nanocomposite were determined using scanning electron microscopy. The electrochemical immunosensor for anti-tTG antibodies was prepared by immobilizing transglutaminase antigen (tTG-antigen) onto the GNP|OvoxPpy||GCE by drop coating and allowed to incubate for 2 hrs. The electrochemical characterization of the nanocomposite platform and immunosensor were studied by voltammetry and electrochemical impedance spectroscopy (EIS). Charge transfer resistance, R_{ct} (obtained from EIS data fitting) of $[Fe(CN)_6]^{3-/4-}$ redox probe was used as the analytical parameter for measuring the interfacial kinetics which occurred as a result of the bio-recognition event (affinitive binding) between the tTG-antigen and anti-tTG antibody. R_{ct} was found to increase with increased

concentration of the antibody as a result of the reluctance to the flow of redox probe charge across the interface. Antibody concentration as low as in 1:4000 dilutions was detected.

DECLARATION

I declare that *Nanocomposite immunosensor for anti-transglutaminase antibody* is my own work, that it has not been submitted before for any degree or examination in any other university, and that all the sources I have used or quoted have been indicated or acknowledged as complete references.

Natasha West November 2009

Signed …….

ACKNOWLEDGEMENTS

I would like to express my sincere gratitude to the following people, without whom this thesis would not have been possible.

My supervisors Profs E. I. Iwuoha and P. G. L. Baker for your guidance and the opportunity to work in the SensorLab research group.

Chemistry Department staff, for technical and academic assistance.

SensorLab colleagues, especially to **Dr. Omotayo Arotiba,** thank you for the insight and guidance you have given me. I am delighted to work with such wonderful people.

My mother, for giving me the freedom and opportunities to explore my dreams, and for all your personal sacrifices to ensure my success. Thank you for always being my source of encouragement which has often kept my sails full of wind and destiny.

Hillmar Ross, for your love and prayers. Thank you for sharing my struggles, joys and dreams and for being a source of encouragement through all the tough times.

Beverly Jakobs, for being such a wonderful friend and for always being willing to help whenever I needed you, especially during those times I had to burn the midnight oil.

My family, for showing interest in my research work and supporting me throughout my years of study.

Nicolette Hendricks, for your kind and loving heart and thank you for always being willing to help in the best way you can.

The National Research Foundation (NRF)/ Department of Science and Technology (DST), for awarding me a DST Innovation Scholarship for MSc and funding my research through the South Africa-Spain Collaboration Grant of Prof Emmanuel Iwuoha (SensorLab, University of Western Cape, South Africa) and Prof Ciara O'Sullivan (Nanobiotechnology and Bioanalysis Group, Universitat Rovira i Virgili, Spain).

My Heavenly Father, You are the reason for my success. Your power was made perfect in my weakness and when challenges seemed insurmountable, your grace has been sufficient.

LIST OF FIGURES

	Title	Page
Figure 1:	Important attributes of an antibody	**34**
Figure 2:	Common circuit models for (a) non-Faradaic and (b) Faradaic interfaces. (c) non-Faradaic impedance data in Nyquist representation (d) Faradaic impedance data in magnitude/phase (bode plot) representation.	**62**
Figure 3:	Typical cyclic voltammogram for a reversible process.	**64**
Figure 4:	Polymerization process of 0.15 M pyrrole monomer in 0.1 M $LiClO^-$ at +800 mV for 120 s	**69**
Figure 5:	Overoxidation of polypyrrole in 0.1 M NaOH for 400 s	**70**
Figure 6:	CV of Gold Nanoparticles deposition onto OvoxPpy||GCE	**70**
Figure 7:	(a) SEM of the ClO_4^- doped plainly formed conductive polypyrrole film. (b) SEM of the overoxidized polypyrrole-film on the GCE, OvoxPpy||GCE. (c) SEM of the gold nanoparticles electrodeposited on the bare glassy carbon electrode, GNP||GCE. (d) SEM of the GNP|OvoxPpy||GCE composite film, (e) SEM micrograph of a selected segment of the GNP|OvoxPpy||GCE composite	**74**
Figure 8:	CV of the bare GCE (c), the overoxidized polypyrrole film (a) and the gold nanoparticles overoxidized polypyrrole composite film (b). **Inset**: Forward and reverse square waves of the overoxidized polypyrrole film and the gold nanoparticles modified overoxized polypyrrole composite film at 5 Hz.	**75**

Figure 9: Shows the square wave curves (SW) of GNP|OvoxPpy||GCE (a) and OvoxPpy||GCE (b) in PBS (pH=7.01) at 50 mV/s. **76**

Figure 10: CV of the GNP|OvoxPpy||GCE. Recorded in argon saturated PBS (pH 7.4) at increasing scan rates (10-700 mV/s) versus Ag/AgCl **76**

Table 11: Plot of the dependence of peak currents on scan rate **77**

Figure 12: **(A)** Cyclic Voltammogram of 0.001 M Fe $(CN)_6^{3-}$ in 1.0 M KCl at bare (a), OvoxPpy||GCE (b), GNP|OvoxPpy||GCE (c). Scan rate: 50 mV/s **80**

(B) Cyclic Voltammogram of 0.001 M Ru $(NH_3)_6^3$ in 0.1 M PBS (pH 7.0) at bare (a), OvoxPpy||GCE (b), GNP|OvoxPpy||GCE (c). Scan rate: 50 mV/s.

Figure 13: Electrochemical impedance spectrum at various potentials (0-400 mV). **(A)** Bode plot. **(B)** Nyquist plot. **82**

Figure 14: The influence of time **(A)** and temperature **(B)** on the response of the immunosensor **84**

Figure 15: **(A)** Nyquist plot of the Faradaic impedance measurements of the GCE after the different incubation steps. Measurements were performed in 2.5 mM Fe $(CN)_6^{3-/4-}$ redox probe, within a frequency range from 100 mHz to 100 kHz. (1) The GNP|OvoxPpy||GCE. (2) Electrode after transglutaminase immobilization. (3) Electrode after blocking with BSA. (4) Immunosensor after incubation with an anti-transglutaminase antibody solution. **88**

(B) Bode Plot of data points measured for the GCE after each different

incubation steps. Measurements were performed in 2.5 mM Fe $(CN)_6^{3-/4-}$ redox probe, within a frequency range from 100 mHz to 100 kHz.

Figure 16: **(A)** Nyquist plot of the immunosensor with different anti-transglutaminase antibody concentrations. Measured in 2.5 mM Fe $(CN)_6^{3-/4-}$, within a frequency range of 100 mHz to 100 kHz. **91**

(B) Calibration graph describing the relationship between the charge transfer resistance ΔR_{ct} and different dilutions of the anti-transglutaminase solutions.

Figure 17: Calibration graph showing the deviation in correlation between the charge transfer resistance and impedance values obtained at 890.3 mHz and 10.3 Hz. **93**

Figure 18: **(A)** Nyquist plot showing the stability of the immunosensor **95**

(B) Linear plot showing the change in R_{ct} over a period of 5 days

Figure 19: Bode Plot of data points measured for the GNP|OvoxPpy||GCE (1) tTG antigen immobilization (2), BSA Blocking (3) and PBS (Blank) incubation (4). **97**

Figure 20: Bode Plot of data points measured for the GNP|OvoxPpy||GCE (1), BSA Blocking (2) and tTG antibody immobilization (3). **97**

Figure 21: Bode Plot of data points measured for the GNP|OvoxPpy||GCE (1), BSA Blocking (2). **98**

LIST OF TABLES

	Title	Page
Table 1:	Summary of parameters for diagnosis of reversible, irreversible and quasi reversible cyclic voltammetric processes.	**65**
Table 2:	Characterization of the different sensor phases in Fe $(CN)_6^{3-/4-}$ redox probe.	**89**
Table 3	EIS fitted data for kinetic index of the immunosensor with different antibody concentrations	**89**
Table 4:	Results of the fitting procedure using impedance values measurement over the whole frequency range and from two selected frequencies from, performed in 2.5 mM Fe $(CN)_6^{3-/4-}$.	**92**
Table 5:	Results of the fitting procedure for control experiments performed. Measurements were performed in 2.5 mM Fe $(CN)_6^{3-/4-}$ redox probe, within a frequency range from 100 mHz to 100 kHz.	**99**

LIST OF SCHEMES

	Title	Page
Scheme 1:	Research framework	**6**
Scheme 2:	Procedure of ion exchange behavior of conducting polymer	**9**
Scheme 3:	The anionic synthesis of polypyrrole from pyrrole monomer	**10**
Scheme 4:	The representation of the polypyrrole overoxidation process	**13**
Scheme 5:	Cross-linking reaction of transglutaminase antigen	**19**
Scheme 6:	The mediation of electron transfer process	**27**
Scheme 7:	Principle of operation of an immunosensor	**28**
Scheme 8:	Antigen-antibody affinity interactions	**36**
Scheme 9:	Schematic representation of the stepwise immunosensor fabrication process	**51**

ACRONYMS AND ABBREVIATIONS

GCE	Glassy carbon electrode
$I_{p,c}$	Cathodic peak current
$I_{p,a}$	Anodic peak current
GNP	Gold nanoparticles
Ppy	Polypyrrole
OvoxPpy	Overoxidized polypyrrole
BSA	Bovine serum albumin
$E_{p,c}$	Cathodic peak potential
$E_{p,a}$	Anodic peak potential
CV	Cyclic Voltammetry
EIS	Electrochemical impedance spectroscopy
CD	Coeliac disease
tTG	Transglutaminase antigen
anti-tTG	Anti-Transglutaminase antibody
SWV	Square Wave Voltammetry
PBS	Phosphate buffer saline
GF	Gluten Free

TABLE OF CONTENTS

ACKNOWLEDGEMENTS _____ *vi*

LIST OF FIGURES _____ *viii*

LIST OF SCHEMES _____ *xii*

ACRONYMS AND ABBREVIATIONS _____ *xiii*

CHAPTER 1 _____ *1*

1.0 BACKGROUND _____ *1*

1.1 Introduction _____ **1**

1.2 Problem Identification _____ **3**

1.3 The Aims of the Research _____ **4**

1.5 Research Framework _____ **5**

CHAPTER 2 _____ *9*

2.0 Literature Review _____ *9*

2.1 Polypyrrole films and their Significance _____ **9**

2.2 The role of doped/undoped polypyrrole _____ **11**

2.3 Overoxidation of Polypyrrole _____ **12**

2.4 Gold colloidal nanoparticles for enzyme stabilization _____ **14**

2.4.1 Preparation and stabilization methods for gold colloidal nanoparticles (GNPs) _____ 15

2.5 Coeliac Disease: an autoimmune disorder _____ **16**

2.5.1 Diagnostic Methods _____ 17

2.5.3 Transglutaminase (tTG) antigen: the autoantigen of CD _____ 18

2.5.4 Anti-transglutaminase antibody: analytical marker for diagnosis of CD _____ 19

2.5.4.2 Immobilization and non-specific adsorption of proteins _____ 21

2.5 Biosensors _____ **23**

2.6.1.1 Electrochemical biosensors _____ 24

2.6.1.1.1 Potentiometric biosensors _____ 24

2.6.1.1.2 Impedimetric biosensors _____ 24

2.6.1.1.3 Amperometric biosensors _____ 26

2.7 Electrochemical Immunosensor _____ **27**

2.7.1 Enzymes _____ 29

2.7.2 Antibodies _____ 30

2.7.3 Antibodies-Production and Properties _____ 31

2.7.3.1 The immune system _____ 31

2.7.3.2 Antibody Structure _____ 32

2.7.3.3 Antibody Antigen Interaction-Affinity _____ 34

2.8 Immobilization methods of biomolecules _____ **36**

2.8.1 Physical Adsorption _____ 37

2.8.2 Entrapment _____ 38

2.8.3 Encapsulation and Confining 39
2.8.4 Covalent Binding 39
2.8 .5 Cross-linking 41
2.8.6 Practical considerations 41

2.9 Conductive electroactive Polymers **42**
2.9.1 Polypyrrole utilized as platform in electrochemical immunosensors 42
2.9.1.1 Polypyrrole utilized as electroactive binding layer 44
2.9.2 Effect of film thickness on cation permselectivity at overoxidized polypyrrole film 45
2.9.3 Polypyrrole utilized in label-free impedimetric immunosensors 46

CHAPTER 3 ***48***

3.0 Experimental Methods of Investigation ***48***

3.1 Introduction **48**

3.2 Materials **48**

3.3 Buffers and solutions **48**

3.4 Electrode Surface Modification **49**
3.4.1 Preparation and stabilization method for gold colloidal nanoparticles (GNPs) 49
3.4.2 Preparation of tTG|GNP|OvoxPPy||GCE 49
3.4.3 Antibody preparation 51

3.4.5 Choice of potential window for EIS **52**

3.4.6 Stability studies **52**
3.4.7 Electrochemical Characterization of Antigen-GNP|OvoxPpy||GCE 52
3.4.8. Scanning Electron microscopy (SEM) 53

Methodology ***54***

3.5 Analytical techniques **54**

3.5.1 Electrochemical impedance spectroscopy (EIS) characterization **54**

3.5.2 Electrochemical Impedance measuring parameters **55**
3.5.2.1 Electrodes 56
3.5.2.2 Instrumentation in Electrochemical Impedance spectroscopy 57
3.5.2.3 Faradaic vs. Non-Faradaic 57
3.5.2.4 Data Fitting 57
3.5.2.5 Circuit Models 58
3.5.2.6 Constant Phase Element 59
3.5.2.7 Double Layer Capacitance 60

3.6 Cyclic Voltammetry **62**

3.7 Square wave voltammetry **65**

2.8 Scanning electron microscopy (SEM) **66**

CHAPTER 4 ***67***

4.0 RESULTS AND DISCUSSION 1 ***67***

4.1 Preparation of overoxidized polypyrrole (OvoxPpy) on glassy carbon electrode **67**

4.2 Electrodeposition of gold nanoparticles on the OvoxPpy||GCE **69**

4.3 Morphological characterization of the electrode assembly 71

4.4 Electrochemical characterization of the modified electrode in PBS 74

4.5 Electrochemical characterization of the modified electrode in Fe $(CN)_6^{3-/4-}$ and $Ru(NH_3)_6^{3+}$ redox probes. 78

5.0 RESULTS AND DISCUSSION 2 *81*

5.1 Choice of potential for EIS 81

5.3 Characterization of the immunosensor with transglutaminase antibody concentrations in Fe $(CN)_6^{3-/4-}$ redox probe. 85

5.4 Sensor with different antibody concentrations 90

5.6 Storage stability of the immunosensor 94

CHAPTER 6 *100*

6.0 CONCLUSIONS AND RECOMMENDATIONS *100*

6.1 Conclusions 100

6.2 Recommendations 101

CHAPTER 1

1.0 BACKGROUND

1.1 Introduction

Among the different types of immunosensors that enable the direct monitoring of label-free affinity-based interactions, electrochemical immunosensors, have received special attention since they possess a number of attractive characteristics, such as, low cost of electrode, mass production, cost effective instrumentation and the ability to be miniaturerized and integrated into microprocessor-controlled diagnostic tools. Based on these attractive characteristics, electrochemical impedance spectroscopy (EIS) based sensors are considered as excellent candidates for clinical and point-of-care diagnostic biomarkers. Among various conducting polymers, polypyrrole has been considered a useful material for immunosensing application, due to their high chemical stability, compatibility with immunoactive entities and facility to be used as matrix for deposition of nanoparticles [1] [2] [3] [4]. In the label free approach, the electrochemical signal observed is solely due to the electrochemical, and electronic or surface properties changes of the immobilised antigen or antibody as it interacts with the target molecule. However, label-free micro-immunosensors are still faced with major challenges, such as, label free biosensors based on hybridisation are argued to have lower detection limit and suffer from interferences due to non specific binding [5]. To overcome this problem, several strategies are employed to enhance the immobilization of the biorecognition components, including the incorporation of nanoparticles [6] [7] [8] [9], the use of porous material to enlarge effective electrode surface area [10] [11], and the orientation-controlled antigen

immobilization techniques [12]. Furthermore, it was found that the sensitivity and selectivity of polypyrrole can be further enhanced by overoxidation and imbedding metal nanoparticles into the porous polymer matrix to form a metal-polymer-composite [13] [14]. The current dissertation describes the application of overoxidized polypyrrole and gold nanoparticles as a Noval matrix for the development of a label-free impedimetric immunosensor with the antigen transglutaminase as the immobilized biological component. The overall emphasis of the immunosensors was for fast and accurate detection of anti-transglutaminase antibodies in low concentration, which can ultimately be utilized as a coeliac disease-marker. Electrochemical impedance spectroscopy (EIS) is a powerful method for the characterization of bulk and surface properties. This technique has already found application for analytical purposes for example, the characterization of protein immobilization on electrodes [15] and for the determination of affinity based antigen-antibody interactions [12]. For EIS measurements, small AC voltage signal perturbations of different frequencies are applied to the system and the current response is determined [16]. Hence, by applying cyclic voltammetry and impedance spectroscopy, the qualitative picture of antigen-modified polymer platform during reaction with an antibody can be achieved.

1.2 Problem Identification

Coeliac disease (CD) is known to be a common genetic disorder; with 1 in every 133 people being positively diagnosed. People with CD have higher than normal levels of certain autoantibodies in their blood. These autoantibodies attack the body's own cells, tissues, and organs, causing inflammation and damage. Coeliac disease is the most common cause of malabsorption, and this inability to absorb sufficient levels of nutrients causes many of the common symptoms experienced by coeliac patients such as chronic diarrhea, fatigue, iron-deficient anemia and osteoporosis. These lead to an increase in mortality rate. However, recognizing coeliac disease can be difficult because some of its symptoms are similar to those of other diseases. As a result, coeliac disease is commonly under diagnosed or misdiagnosed. Moreover, the longer a person goes undiagnosed and untreated, the greater the chance of developing the refractory case of CD thus leading to the development of T-cell lymphoma, which is the primary cause of morbidity and mortality [17].

The current diagnostic tests for CD include a particular series of blood tests called the 'Coeliac panel' screening, and a small bowl biopsy. These methods however, suffer from distinct disadvantages which include being every complex, extremely tedious and require skilled operators. Furthermore, these methods are expensive and are not designed to give rapid analysis, thus inevitably lowering the quality of life for the patient. As part of the solution to the demands for point-of-care measuring devices, this work aims at developing an affordable immunosensor for the rapid quantification and accurate detection of anti transglutaminase antibodies in low concentrations to aid in point-of-care analysis.

1.3 The Aims of the Research

Based on the preceding section, the following aims and objectives have been identified:

To electropolymerize pyrrole on a glassy carbon working electrode.

To electropolymerize characterize both polypyrrole and overoxidized polypyrrole for the application as an immobilization platform of the tTG antigen.

To immobilize and incubate the transglutaminase antigen on the electrode.

To evaluate the platform and immunosensor performance using cyclic voltammetry and electrochemical impedance spectroscopy.

To develop an impedimetric Immunosensor for detection of low anti-transglutaminase antibody concentrations based on Overoxidized-polypyrrole/gold nanoparticles composite.

1.4 Rationale and Motivation

Conventional methods for coeliac disease diagnostics and quantification of anti-transglutaminase antibodies include; serological blood tests with additional biopsies of the duodenum antibody testing, screening and detecting pathological changes in the small bowel of coeliacs. Serological testing can aid in the diagnosis of coeliac disease. However, it is less sensitive and specific than small bowel biopsy and cannot be relied on alone to make the diagnosis. The current methods of diagnosis are expensive and tedious and also needs the assistance of professional personnel. Therefore, smaller, faster and cheaper devices are highly desired for replacement of time-consuming laboratory-analysis.

The presence of tTG antibodies is highly suggestive of CD. Direct measurement of anti-tTG to tTG-antigen can now be done by immunoassay methods which are capable of direct and specific detection of proteins and peptides in 'real' samples, like serum and plasma. In most immunosensors, the antibody is immobilized onto a conductive support, and the electrical properties of the interface are modified when the antibody reacts with the antigen of interest. The prior literature survey information exemplified the fact that tedious methods of continuous serological blood tests for antibodies, particular tTG-antibodies together with a lifelong GF diet, is an absolute necessity to ensure effective treatment, whilst concomitantly reducing mortality. Hence, the superior method for executing the task was shown to be label-free impedimetric immunosensors, in which appropriate miniaturization of bio-affinitive and transducer components for adequate antigen-antibody interaction, is expected to allow for fast and accurate diagnosis. Considering these aspects, the motive for the current study was thus established.

1.5 Research Framework

My thesis was designed to follow some sequential steps which were optimised over time. In line with the study objectives and the experimental procedure, a broad research design can be summarised in the flow diagram below:

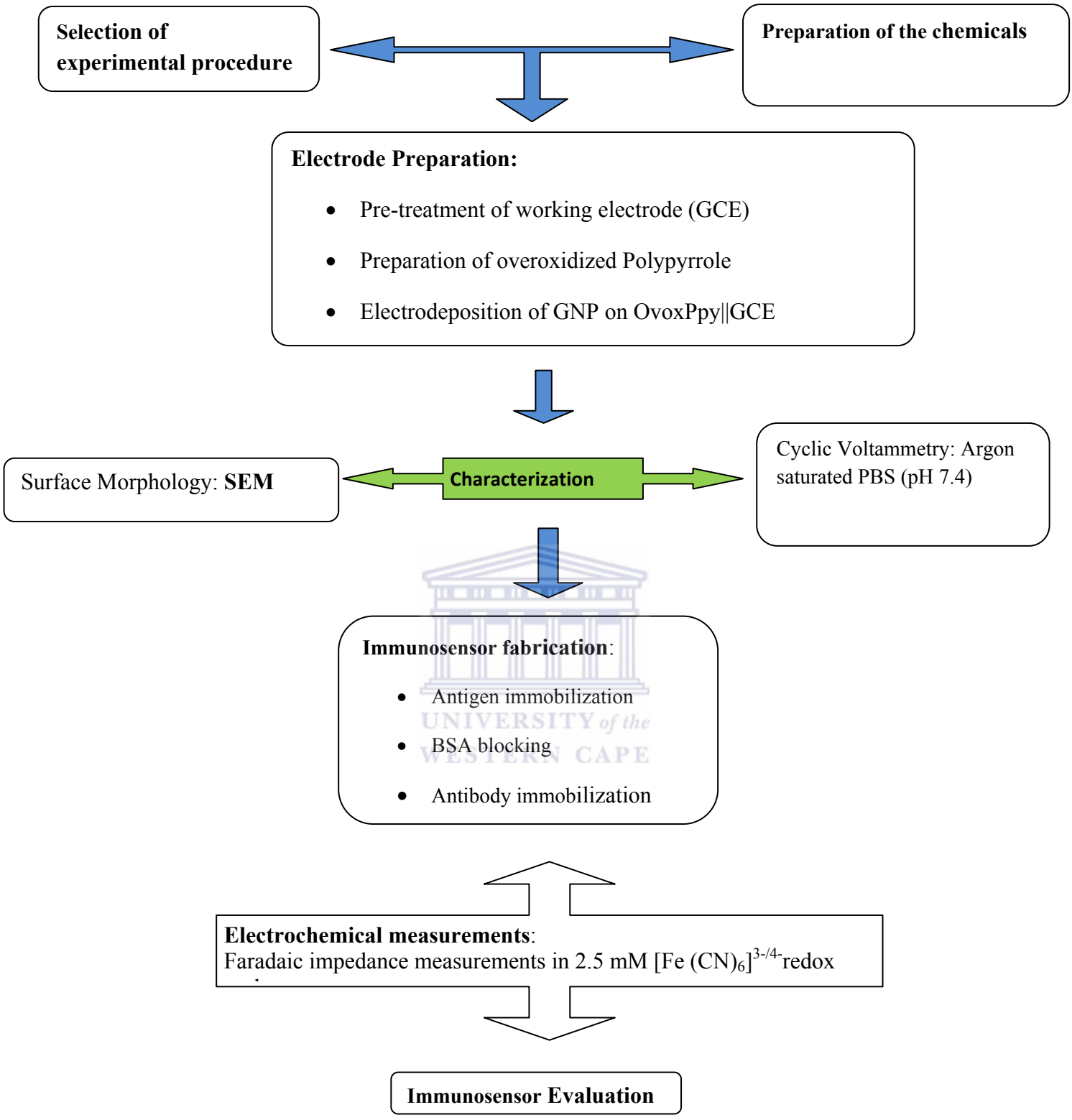

Scheme1: Research framework

1.6 Outline of the thesis

The thesis will be presented as outlined briefly below:

An introduction giving various aspects that contributes to the increased mortality rate with regard to undiagnosed or misdiagnosis of CD and the importance for adequate and continuous health assessment are raised in this chapter. Coeliac disease analysis, the disadvantages associated with current diagnostic methods, the risk associated with long-term undiagnosed CD and the need for developing immunosensors for fast and accurate diagnosis of CD are also highlighted. The use and advantages of polypyrrole and gold-nanoparticles that can possibly lead to fabrication of the immunosensor platform in this study are discussed. The objectives of this study, work frame and delimitations of this study are also discussed in this chapter.

A literature review relating to polypyrrole, the role of doped/undoped polypyrrole and overoxidized polypyrrole will be presented in Chapter 2. Furthermore, the various aspects of biosensors, biomolecules as well as, immobilization methods are presented in Chapter 2. This chapter also covers a brief introduction to conducting polymers containing metals as well as, an introduction to overoxidized polypyrrole as matrix for uniform incorporation of Au-nanoparticles and its use as immobilization platform. Characterization methods, mainly electrochemical impedance spectroscopy, cyclic voltammetry, square wave voltammetry and scanning electron microscopy are also briefly discussed in this chapter. In Chapter 3, information regarding the chemicals used, instrumentation and research design with an overview of all the sequential steps taken to solve the thesis problem are described.

In Chapters 4 and 5 results are presented and discussions are offered. Chapter 4 focuses on the characterization of the developed nano-composite modified electrode, whereas, Chapter 5 highlights the immunosensor response after each consecutive incubation step based on electrochemical impedance spectroscopy. In addition, a detailed description of the immunosensor and its analytical characteristics such as stability, detection limit, selectivity, linear range and reproducibility is presented. This chapter also features the results and discussion of the developed immunosensor response to various antibody concentrations.

Finally, Chapter 6 presents the conclusions.

CHAPTER 2

2.0 Literature Review

2.1 Polypyrrole films and their Significance

Ion exchange behavior during the charging and discharging process of conducting Polypyrrole (PPy) has been widely studied in recent years. The ability of polypyrrole to switch between oxidized and reduced states leading to its conducting and insulating properties is also gaining great interest [18].

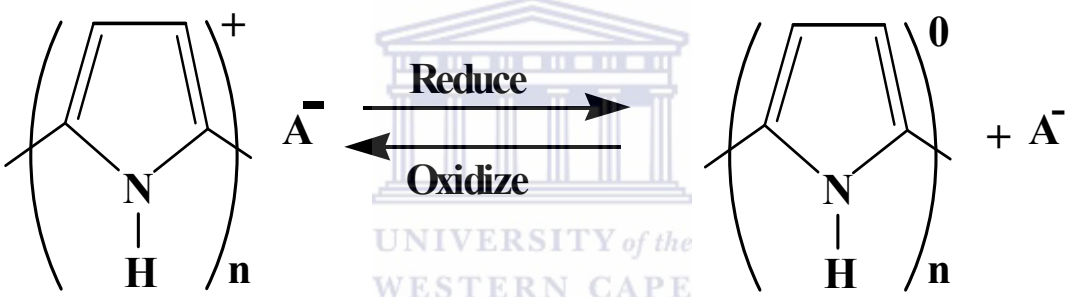

Scheme 2. The ion exchange behavior of conducting polymer by doping with oxidizing agent (p-doping) or reducing agents (n-doping).

It has been found that conducting polymers exchange anions as well as cations, depending on the polymerization conditions, type and size of the incorporated counter-ions, ions present in the electrolyte solution, polymer thickness and ageing of the polymer [19]. Conducting polymers can be prepared by chemical or electrochemical polymerization. During the chemical polymerization process, monomers are oxidized by oxidizing agents or catalysts to produce conducting polymers. The electrochemical method involves the direct formation of conducting polymers with better control of polymer film thickness and morphology; by

varying the potential or current with time, thus making them suitable for use in electronic devices. Electrochemical synthesis is becoming the preferred method for preparing electrically conducting polymers due to its simplicity and reproducibility. An advantage of electropolymerisation is that the reaction can be carried out at room-temperature.

Chemical bonding in conducting polymers provide one unpaired, π-electron per carbon atom in the backbone of the polymer. Carbon atoms are in sp^2p configuration in the π-bonding and orbital's of successive carbon atoms overlap; providing delocalization of electrons along the backbone of the polymer. The delocalization provides the charge mobility along the backbone of the polymer chain and induces electrical conductivity and high electron affinity.

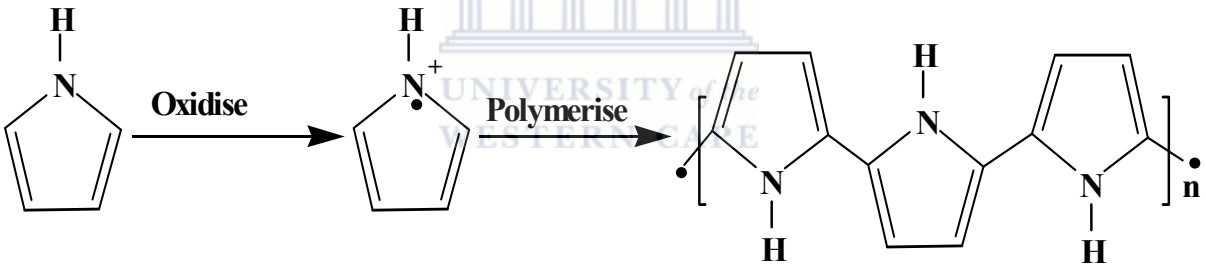

Scheme 3. The anionic synthesis of polypyrrole from pyrrole monomer.

In the oxidation form, the cationic product contains a staggered, conjugated π-electron network that can be balanced with dopant ions such as ClO^-_4, which provide different electrochemical and mechanical properties to the polymer. During the polymerization process cations from electrolyte are expected to exhibit electrostatic repulsion forces with radical cations of pyrrole monomers. This repulsion forces largely depend on the charge of cations.

Lithium ions having larger effective charge due to localization of charge in a small size will readily expel the radical cations of pyrrole monomers out of the region where precipitation of the intermediate occurs. Hence, the coupling change of radical cations with each other becomes smaller due to repulsion forces between the lithium ion and radical cations. Generation of radical cations in the region of the base electrode is much larger in the potentiostatic polymerization and it is hard to retain the electrolytic cations because the electrode maintains constantly at a higher positive potential. Prior literature established that current decrease indicates mass increase at the electrode. The applied potential sufficient to oxidize the pyrrole monomers allow for continues mass increase. This indicates that electrochemical growth of polymer is very much dependent on the applied potential.

2.2 The role of doped/undoped polypyrrole

Amongst the studied conducting polymers, Polypyrrole (Ppy) has attracted considerable attention and has found significant application in batteries, sensors, metal protection against corrosion and molecular imprinted sensors [20]. This polymer can be easily prepared by electrochemical oxidation of the monomer in the presence of suitable dopant ions. The general properties of polymers depend on various factors, such as the electrical potential, the current density used, the concentrations of the reactants, solvent nature, electrode substrates, etc.[21]. However, structural characteristics within polymer are easily affected and therefore, depending on the envisioned application, careful choice of dopant ions and polymerization conditions during polymer synthesis are also of pivotal importance. One of these changes associated with irreversible processes is the loss of conductivity through overoxidation, where the dopant ions are expelled from the backbone of the polymer. However, overoxidized-polypyrrole (OvoxPpy) is an excellent material used as a matrix for the

deposition of metal nanoclusters, since it consist of nano-pores within the polymer film. The unique properties of Au nanoparticles namely, good conductivity, useful electrocatalytic and biocompatibility, makes Au nanoparticles to be considered excellent material for fabrication of electrochemical sensors and biosensors. The immobilization of enzyme to solid electrode surface is a crucial step for the fabrication of biosensors [22]. Usually, the methods include direct physical adsorption onto a solid support [23], encapsulation into hydrogel[24], cross-linking [25], and covalent binding [26]. A key requirement of enzyme immobilization is attachment of the enzyme without the bioactivity being sacrificed [27]. In particular, the immobilized film needs to be resistant to a wide range of physiological pH's, maintaining their stability and activity with change in temperature, ionic strength and chemical composition. In this regard the application of conducting polymers has been a hot research topic because they exhibit various physical and chemical phenomena, such as bending and volume change in the presence of external stimuli (change in pH, solvent composition, ionic strength, and temperature). The catalytic activity of the OvoxPpy film can be significantly enhanced by the incorporation of Au nanoparticles, due to increasing electronic conductivity and increase in effective surface area. In this regard the GNP|OvoxPpy modified film platform provides an attractive template for enzyme immobilization.

2.3 Overoxidation of Polypyrrole

Polypyrrole undergoes overoxidation at positive potentials, and/or in more alkaline media; this is regarded as an undesirable degradation process, which leads to the loss of conductivity and dedoping [28]. During this process, dopant anions are expelled into the solution phase leaving the polymer in its neutral non-conductive state, thus making it susceptible to nucleophilic attack. Furthermore, some literature reviews have pointed out that in aqueous

media, the Ppy overoxidation potential depends on the solution pH, the higher the pH the lower the overoxidation potential. Indeed, the Ppy overoxidation process is more effective in basic solution (NaOH) than in NaCl solution [29]. In sodium hydroxide solution, the overoxidation of the polypyrrole film proceeds faster than in median pH buffered solutions because hydroxide ions act as nucleophilic reactants which are stronger than the anionic species present in buffer solutions [30].

The overoxidation of polypyrrole, results in higher density carbonyl groups (>C=O and $-COO^-$) being generated along the polymer backbone which favors the accumulation of cationic species via ion-exchange equilibrium process and in-turn results in catalytic oxidation of the Ppy-film at the electrode. The existence of dense carbonyl groups on the backbone of OvoxPpy film can provide a selective interface for binding interactions between the OvoxPpy surface and the immobilized biomolecule.

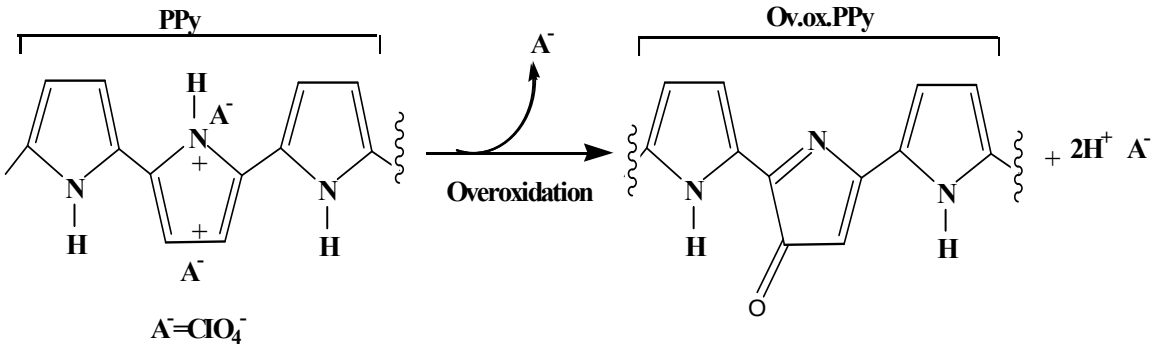

Scheme 4. The overoxidation of polypyrrole from basic solutions.

Prior research has confirmed that overoxidation of polypyrrole is initiated by hydroxyl radicals formed due to the oxidation of water, of which the overall process may be described by equation 1:

$$\mathbf{Ppy + xHO\text{-} \rightarrow OvOxPpy + ne^{-} + mH^{+}\ \ldots} \qquad \ldots. (1)$$

2.4 Gold colloidal nanoparticles for enzyme stabilization

The application of colloidal gold in immunoassays date back to the early 1970s when 5-50 nm colloidal gold particles were first used as electron-dense probes in electron microscopy and thus enabled sensitive, high-resolution immunochemistry [31]. Because of the intrinsic electrochemical characteristics of gold, colloidal gold was introduced into the research field of electrochemical immunosensors and immunoassays. Colloidal gold nanoparticles (GNP) can play an excellent role in the immobilization of biomolecules, because they provide an environment similar to that of biomolecules in their native system. Numerous investigations have shown that several enzymes maintain their enzymatic and electrochemical activity when immobilized on gold nanoparticles.

Colloidal gold provides a very high surface to volume ratio. Moreover, the presence of GNPs gives immobilized protein molecules more freedom of orientation, and as such, permit proteins to orient in conformations more favorable for direct electron transfer, with the active site being closer to the conducting electrode [32]. Colloidal gold particles form the conducting electrode and are thus the site of electron transfer when anchored to the substrate. It is believed that the nanoscaled contours of the correctly sized nanoparticles can penetrate slightly into the protein, lowering the electron-transfer distance between the electrode and the

redox site embedded in the protein thus, facilitating the electron transfer through the conducting tunnels of colloidal gold[33].

2.4.1 Preparation and stabilization methods for gold colloidal nanoparticles (GNPs)

The first step for the synthesis of GNPs is the reduction of Au (III) involving the use of $HAuCl_4$ in the presence of KCl. The most popular method used for synthesis of GNP, is based on chemical methods, which involves the reduction of metal salts; however, a stabilizing agent is always required to prevent the aggregation of colloids into larger particles. Known stabilization methods include, (i) electrostatic stabilization, using ionic compounds, such as halides, carboxylates or polyoxoanions dissolved in solution; (ii) steric stabilization using macromolecules, such as polymers or oligomers – the adsorption of these molecules at the surface of these particles will provide a protective layer, and (iii) electrosteric stabilization, by means of ionic surfactants.

An important aspiration for biosensor design is that, the biological film be adaptable to various environments. In particular, the immobilized films must be stable over a wide range of physiological pH's, maintain their stability and activity with changes in temperature, ionic strength and chemical composition. Hence, there is a need to design platforms that are compatible with the biological component and which can affect rapid electron transfer at the electrode surface. In this regard, conductive polymers are attractive matrixes for incorporating nano-materials for biosensor applications.

2.5 Coeliac Disease: an autoimmune disorder

CD is an intestinal disorder caused by intolerance to gluten proteins of wheat. These proteins, also known as prolamins, are rich in the amino acids proline and glutamine,[34]. The high proline content of gluten gives it an unusual level of digestive resistance against the gastropancreatic and brush border membrane proteases and peptidases that typically hydrolyses food into tripeptidases, dipeptidases, or single amino acids in the small intestine [35]. Therefore, when peptides of sufficient length penetrate a considerable distance into the lumen of the small intestine it triggers a T cell-mediated immune response. Prior to causing inflammation, these metastable peptides are regiospecifically deamidated by the enzyme transglutaminase. Deamidated gluten peptides have a considerable increased affinity for the major histocompatibility complex (MHC) protein HLA-DQ2, which together with HLA-DQ8 is the only known genetic risk factor for developing the disease and is expressed by more than 90% of CD patients [36]. Small intestinal T-cells recognize the gluten peptide-DQ2 complex as a foreign pathogen and orchestrate the ensuing small intestinal inflammatory response. This leads to the flattening of the small intestinal villi thereby significantly decreasing the absorption surface area of the small intestine. The inability to absorb sufficient levels of nutrients causes many of the common symptoms experienced by celiac patients, such as chronic diarrhea, fatigue, iron-deficient anemia, and osteoporosis, and leads to an increase in the mortality rate.

2.5.1 Diagnostic Methods

Up to date, the only treatment for CD involves complete, life-long exclusion of gluten containing foods from the diet. Although this treatment is effective, it is difficult to maintain and lowers the overall quality of life for patients [37]. The recognition that the enzyme tissue transglutaminase is the autoantigen for the development of endomysial antibodies [38], allowed development of automated enzyme-linked immunoassays that are accurate and cost-effective than time consuming laboratory analysis. Recognizing coeliac disease can be difficult because some of its symptoms are similar to those of other diseases. As a result, coeliac disease is commonly under diagnosed or misdiagnosed. Thus, the longer a person goes undiagnosed and untreated, the greater the chance of developing long-term complications. The current diagnostic tests for CD include a particular series of blood tests called the 'Coeliac panel'. These tests measure ones immune system's response to gluten in the food you eat, screening which involves testing for the presence of antibodies in the blood in people without symptoms, and a small bowel biopsy, during which a tiny piece of tissue from the small intestine is removed to check for damage to the villi. People with coeliac disease have higher than normal levels of certain autoantibodies in their blood. Direct measurement of antibody to tTG can now be done by immunoassay methods which are capable of direct and specific detection of proteins and peptides in 'real' samples, like serum and plasma.

It is recommended that the test for anti–tissue transglutaminase antibodies be used as a single screening test for celiac disease [39]. If the levels of this marker are within the normal range (or

if it is absent) and there is a high suspicion of coeliac disease, selective IgA deficiency needs to be ruled by measuring total IgA levels. In such cases, a test for IgG antibodies against tissue transglutaminase should be performed [40].

2.5.3 Transglutaminase (tTG) antigen: the autoantigen of CD

In 1997, the enzyme tissue transglutaminase (tTG) has been reported to be the main, if not sole, target for endomysial antibodies that are characteristic for CD. Based on the later observation, a series of studies have revealed that screening for the presence of tTG-specific antibodies is a very specific indicator for CD. In CD, gluten which is cross-linked to tTG are able to stimulate transglutaminase specific B-cell responses that eventually result in the production of ATA, IgA and IgG antibodies [41]. As an outside membrane-bound protein, tTG cross-links proteins between an ε-amino group of a lysine residue and a γ-carboxamide group of glutamine residue, creating inter- or intramolecular bonds that are highly resistant to protein degradation. The enzyme forms covalent bonds between the γ-carboxyl group of a glutamine residue in one polypeptide chain and a lysyl substrate in a second polypeptide chain with the subsequent release of ammonia (NH_3).

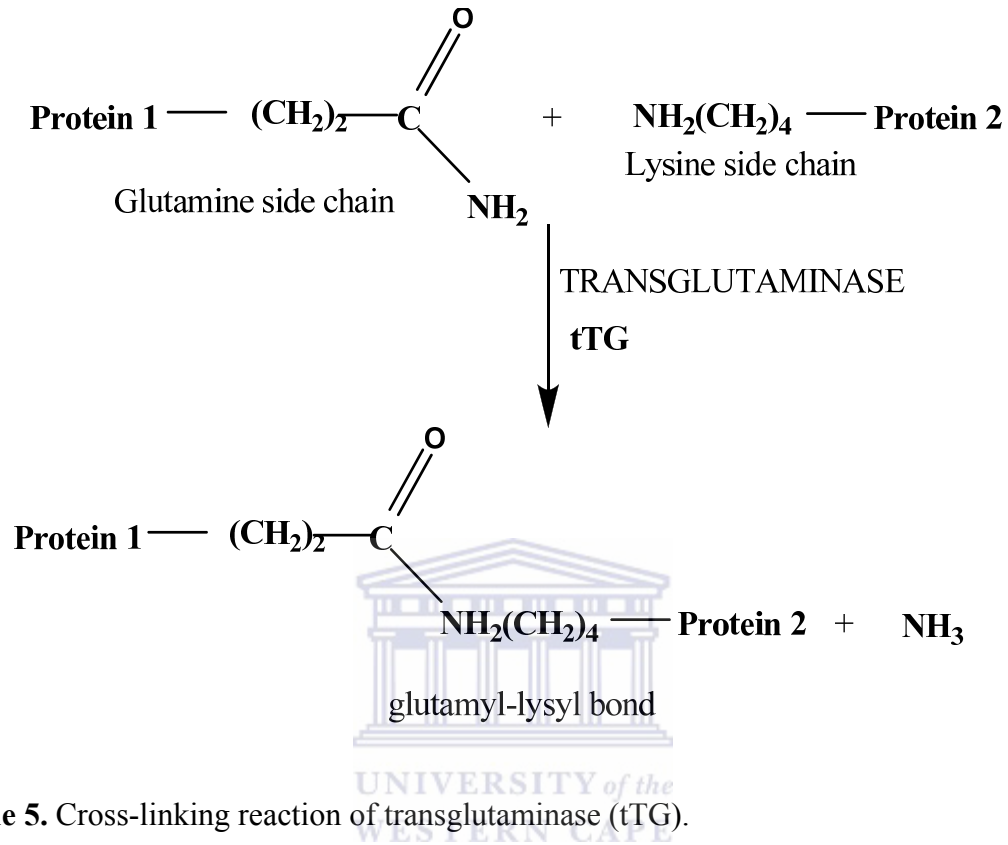

Scheme 5. Cross-linking reaction of transglutaminase (tTG).

2.5.4 Anti-transglutaminase antibody: analytical marker for diagnosis of CD

Anti-transglutaminase antibody concentration fall once a gluten-free diet has begun, thus facilitating monitoring of dietary compliance. Therefore, anti-tTG is a highly sensitive and important serological marker, used to screen patients with suspected coeliac disease, and have a specificity of 90 to 97 % [42].

2.5.4.1 Electrochemistry of antigen modified electrode

An antigen immobilized on the electrode surface identifies and interacts with the antibody of interest, resulting in electrostatic attachment of the antibody to the electrode surface. Therefore, the formation of antigen-antibody complex on the conductive support alters the impedance features of the interface; hence impedance spectroscopy can be used to study the antigen-antibody molecular recognition event by measuring the resistive and/or capacitive change that accompanies this reaction.

The mechanism by which conductive electroactive polymers (CEPs) catalyze antigen-antibody (Ab-Ag) interactions has some technical challenges due to several reasons. Firstly, biochemical process often runs in parallel with charging taking place at the double layer and the mass transport process at the polymer interface. Secondly, problems arise because of the imprecise description of the state of the interface, the electrical variables, and the concentrations of the reactant and product in the reaction medium. Thirdly, the reaction between the Ab and Ag does not involve a redox transfer found typically in the redox transformation of substrate to product at the enzyme-modified CEP electrodes [43]. Based on the latter, it occurs that the mechanism of the Ab-Ag reaction at the CEP-based electrodes involves the variation in the capacitive properties of the polymer. Specifically, the interaction between an antigen and a modified conducting polymer will induce a change in the capacitance of the polymer and produce an analytical signal when measured by electrochemical impedance spectroscopy.

2.5.4.2 Immobilization and non-specific adsorption of proteins

There are a number of requirements that the immobilization technique must satisfy if immunosensors are to be of practical use: (i) the antigen must retain substantial biological activity when attached to the sensor surface; (ii) the biological film must retain tightly associated with the sensor surface whilst retaining its structure and function; (iii) the immobilized biological film needs to have long-term stability and durability; and (iv) the biological material needs to have a high degree of specificity to a particular biological component. These conditions must be satisfied for an efficient sensing device.

The biological material is either immobilized alone, or they are mixed with other proteins, such as bovine serum albumin (BSA), either directly on the transducer surface, or on a polymer membrane covering it. Improvements of biocatalytic efficiency can be achieved by manipulating the structure of the carrier materials for antigen immobilization. Reduction in the size of protein-carrier materials can greatly improve the efficiency of immobilized biomolecules. [44]. In the case of surface attachment, smaller particles can provide a larger surface area for attachment of biomolecules.

Usually, immunosensors are heterogeneous, which indicate that either the antibody or antigen is immobilized on a solid carrier and upon contact with a solution containing the immunoagent an immunocomplex is formed. The unbound proteins are removed by washing and the response obtained is proportional to the amount of protein bound.

Another significant aspect to consider during immunosensor design and fabrication is the presence of a fully inert surface in order to prevent non-specific protein adsorption that may yield a false positive signal. Problems associated with non-specific adsorption are greater where the target is a low concentration protein and where the support may become fully blocked with non-specific proteins, thus preventing the specific adsorption. Therefore, in this study, BSA was utilized as surface blocking agent after antigen immobilization. This method has shown to be feasible to reduce non-specific adsorption and prevent false-positive results [45].

2.5 Biosensors

The utility of a sensor is determined by its selectivity. Hence, the main advantage of biosensors is their high specificity and sensitivity towards biological objects. A sensor consists of two major parts: a system of molecular recognition, referred to as the receptor and a transducer, which converts the biocatalytic response into a digital electronic signal; the transducer part of the sensor is also known as the detector, sensor, or electrode, but the term transducer is preferred to avoid confusion.

Biosensors are self-contained, all parts being packed together in the same unit, usually small, the biological recognition element being in direct spatial contact with the transducing element. The usual aim being to produce an electronic signal which is proportional in magnitude or frequency to the concentration of a specific analyte or group of analytes to which the biosensing element binds [46]. There are two types of biosensors: biocatalytic and bioaffinity-based biosensors. The biocatalytic biosensor uses mainly enzymes as the biological compound, catalyzing and signalling biochemical reaction**.** The bioaffinity-based biosensor is designed to monitor the binding event itself and uses specific binding proteins, lectins, receptors, nucleic acids, membranes, whole cells, antibodies or antibody-related substances for biomolecular recognition. In the latter two cases, these biosensors are referred to as immunosensors.

2.6.1 Types of biosensors

2.6.1.1 Electrochemical biosensors

The underlying principle in this class of biosensors is that many chemical reactions produce or consume ions or electrons which in turn cause some changes in electrical properties of the reaction solution which can ultimately be sensed and utilized as a measuring parameter. Based on the electrochemical parameter measured, electrochemical biosensors can further be classified into amperometric, potentiometric, and impedimetric biosensors.

2.6.1.1.1 Potentiometric biosensors

Also known as ion-selective electrodes (ISEs), these sensors encompass a large subset of electrochemical sensors. In many cases, the potentiometric sensor comprises a membrane with a unique composition, noting that the membrane can be either a solid (i.e., glass, inorganic crystal) or a plasticized polymer, and the ISE composition is chosen in order to impart a potential that is primarily associated with the ion of interest via a selective binding process at the membrane–electrolyte interface. Potentiometric devices rely on the measurement of change in potential that arise from the redox reaction of an analyte with a specific receptor. The principle behind this is that, when a ramp voltage is applied to an electrolyte the electrochemical reaction causes a flow of current. The voltage at which the reaction occurs indicates a particular reaction of a particular species. The most common potentiometric devices are the pH electrodes.

2.6.1.1.2 Impedimetric biosensors

The measured parameter in this type of biosensor is the conductance or resistance of a solution. During electrochemical reactions, ions or electrons are either produced or consumed and this causes an overall change in the conductivity of the solution. This change is measured

and calibrated to a proper scale. In most immunosensors, the antibody is immobilized onto a conductive support, and the electrical properties of the interface are modified when the antibody reacts with the antigen of interest. The surface organization and assembly of antibodies is a critical step in the fabrication of an immunosensor device. Characterizing the immobilization of the antibody along with its stability/activity and interaction with the antigen are important steps in optimising the analytical performance (i.e. selectivity, stability, sensitivity, response time etc) of the immunosensor. The formation of an antigen-antibody complex on a conductive support alters the impedance features of the interface, and impedance spectroscopy is used to study the antigen-antibody molecular recognition event by measuring the resistive and/or capacitive change that accompanies this reaction.

Studies by Corry et al. 2003 showed that EIS is a powerful method for predicting the surface activity of an immunosensor. The impact of immobilization on the antibody-antigen binding event was studied, and it revealed that covalent attachment of an antibody to the electrode surface is needed for a successful impedance-based immunosensor. Cui et al. 2003 used EIS to characterize the growth of a multilayer film that comprised avidin and biotin labelled antibody formed on a mercaptopropionic acid modified gold electrode. It was observed that the electron transfer resistance increases proportionally with the number of avidin/biotin antibody layers. EIS is extremely useful in monitoring the immunosensor surface properties before and after antibody immobilization in a phosphate buffer solution. The generation of a precipitate onto the electrode surface *via* biocatalysis can lead to a substantial increase in the interfacial impedance. An antibody modified indium tin oxide electrode has been used in conjunction with EIS in detection of *Esherichia coli.* Signal amplification was accompanied by using combined redox probe and antibody labelled enzyme (alkaline phosphatase), and it

was demonstrated that the interfacial electron transfer resistance increases at elevated levels of *E. coli*. Similar impedance trends were observed without enzymatic amplification. Zayats et al., 2002 fabricated an ISFET device to monitor antigen-antibody binding processes, and used EIS to follow the thickness of various films formed on the ISFET surface. Betty et al., 2004 fabricated a capacitative immunosensor based on electrolyte insulator porous silicon structures, and employed EIS to characterize the interfacial region after different surface treatments. In most EIS studies, measurements are made over a wide frequency range in order to obtain the various interfacial parameters (charge transfer resistance or double layer capacitance). However, Dijksma et al., 2001 developed an electrochemical immunosensor for the detection of the protein interferon-γ by monitoring the biorecognition event at a single frequency.

2.6.1.1.3 Amperometric biosensors

Enzymes provide an attractive method for signal amplification. The continual turnover of a substrate generates a cascade signal that is large and therefore be measured quite easily. Amperometric biosensors generally use reduction/oxidation (redox) enzyme systems. In the simplest case, a redox enzyme is immobilized by some convenient procedure at an electrode surface. The electrode is held at a fixed potential, adjusted so that electrons arising from an oxidized substrate are transferred to the electrode, and this regenerates the active form of a cofactor for another redox cycle by the enzyme. The specificity of the reaction is determined by the enzyme. Because the rate of the enzymatic reaction at a fixed temperature and pH is directly proportional to the substrate concentration, the current produced at the electrode is proportional to the rate of modification of the substrate by the enzyme **(Scheme 6).**

The rate of an enzymatic reaction is dependent on the temperature, pH, ions, cofactors, and competitive or non-competitive inhibitors present in the reaction medium. Any redox compound present, such as oxygen, ascorbate, thiols or certain drugs interfere with the reaction. To circumvent some of these interference effects, chemical electron-acceptors are used as mediators. Thus, for example, ferrocenes-ferricinium redox system has been used in the mediation of electron transfer from glucose oxidase to graphite electrodes [47].

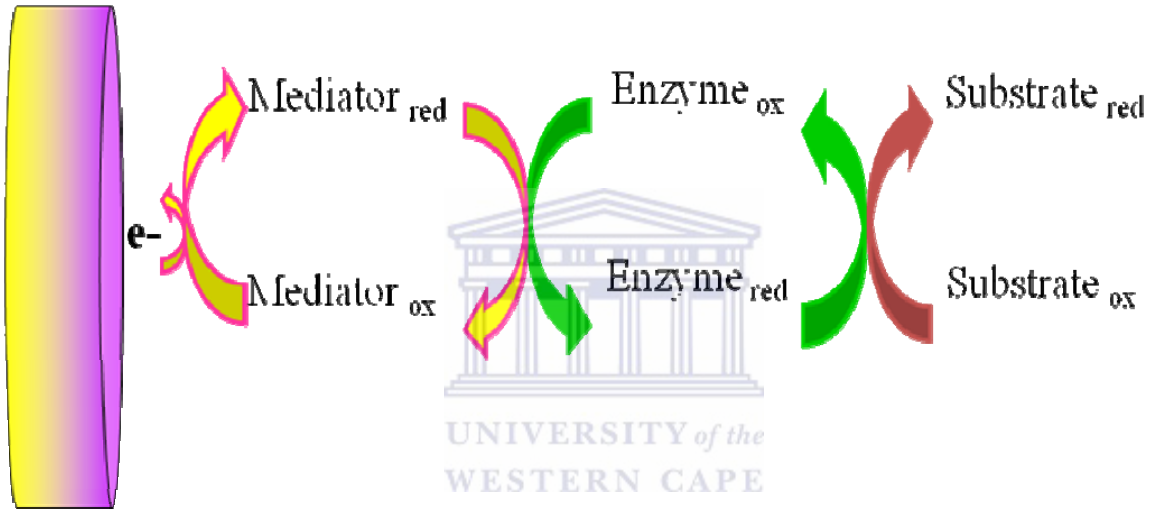

Scheme 6: The mediation of electron transfer

2.7 Electrochemical Immunosensor

Electrochemical immunosensors combine the analytical power of electrochemical techniques with the specificity of biological recognition process, which provides the basis of direct electrical detection of a wide range of analytes with great sensitivity and specificity. Generally, a sensor consists of a sensing element and a transducer. In case of an immunosensors, the sensing element is formed by immobilized antibodies or antigens. In

most studies involving EIS, the antibody-antigen interaction has been monitored *via* a reduction/oxidation reaction that is catalyzed by the use of an electroactive/ redox system i.e., $[Fe(CN)_6]^{3-/4-}$ [48]. The main types of immunosensor detection devices are; electrochemical (potentiometric, amperometric or conductometric/capacitive), optical and microgravimetric. All types can either be described as direct (nonlabelled) or as indirect (labelled) immunosensors. Direct detection without labelling can be performed by cyclic voltammetry, chronoamperometry, impedimetry, and by measuring the current during potential pulses. These methods are able to detect a change in capacitance and/ resistance during the immunocomplex formation, whereas the latter immunosensors use signal-generating labels which allow more sensitive and versatile detection modes when incorporated into the complex.

Scheme 7: Principle of operation of an immunosensor

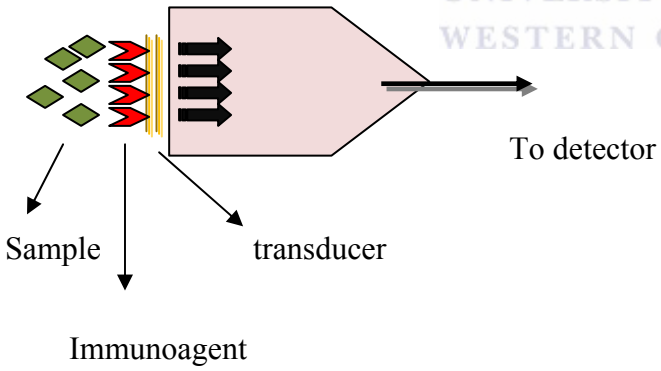

There are a great variety of labels which have been used in indirect immunosensors. The most common enzyme labels include enzymes such as peroxidase, glucose oxidase, alkaline phosphatase (aP), catalase or lucifarase owing to their excellent stability and high turnover

number. Electroactive compounds such as ferrocene or In^{2+} salts, and a series of fluorescent labels (rhodamine, fluorescein, Cy5, ruthenium diamine complexes and phosphorescent porpyhrin dyes) have also been used [49].

2.7.1 Enzymes

Enzymes are biological catalysts responsible for most chemical reactions in living organisms. Their main task is to initiate or accelerate reactions that would otherwise not take place, or only very slowly, at the moderate temperatures predominant in organisms. They also slow down reactions if necessary, or split them up into separate steps, to control the heat evolution of exothermic reactions, otherwise the heat evolution can lead to cell death. Enzymes are the most commonly used biocatalysts in biosensors. Some enzymes such as urease are highly specific for one compound [50]. Other enzymes on the other hand, are specific for a whole group of substrates. The structure of enzymes is mainly made up of a single polypeptide chain, but the active site can be a separate molecule, embedded in the polypeptide backbone. Only certain molecules are allowed access through the protein shell and the binding site, and not the active site itself. When the substrate (S) binds to the binding site of the enzyme (E), a reactive intermediate, the enzyme substrate complex (ES) is formed. The complex ES is converted to E and a product (P) by the active site.

During enzymatic reactions, substrates are consumed and products formed. These compounds can be monitored with suitable transducers. In the case of glucose oxidase, these compounds are O_2 and H_2O_2, which are easily detected. Some enzymes have additional active areas

referred to as co-factors, e.g. NADH. Such co-factors can be used for measuring enzyme activity [50]. Many enzymes also require metal ions for their catalytic activity.

There are two main applications for enzyme in biosensors. They can either be used as catalytic biosensors or as markers in affinity biosensors, such as immunosensors and DNA sensors. In catalytic enzyme sensors, the concentration of enzyme (E) is constant and the substrate concentration is much smaller. When the enzyme is used as a label for antibodies or DNA strands, the substrate must be used in excess and the enzyme concentration (E) is the only limiting factor. Enzymes are sensitive to temperature changes. Increasing temperatures increase the reaction rate, but at elevated temperatures, the protein structure (tertiary structure) denatures, mostly irreversible, leaving the enzyme inactive. For most enzymes, this critical temperature stays between 40 ^{o}C and 50 ^{o}C, however, few enzymes possess high thermal stability above 100 ^{o}C.

2.7.2 Antibodies

The use of highly specific antibodies is very popular. The most important analytical applications of antibodies are immunoassay, immunosensor and immunoaffinity columns. Immunochemical techniques are highly sensitive, selective, simple and inexpensive. They are based on the ability of antibodies to form complexes with corresponding antigens. This interaction is highly specific and leads to very selective immunoassays. The extremely high affinity of the antibody antigen interaction leads to great sensitivity. New antibody technologies such as the production of antibody fragments or recombinant antibodies allow tailoring of the biomolecules for analyte and matrix requirements, within certain limits.

2.7.3 Antibodies-Production and Properties

2.7.3.1 The immune system

Antibodies are produced by mammals as part of an immune response of the host to foreign intruders such as micro-organisms, viruses, bacteria and parasites [51]. The immune system specifically recognises and eliminates pathogens. The first line of defence is innate immunity, a non-specific defence reaction. More important for analytical science is the second line of defence, adaptive immunity. Adaptive immunity is directed specifically against the intruder and is mediated by cells called lymphocytes. The lymphocytes have specific cell surface receptors and secrete proteins which are antibodies that specifically bind to the foreign species (antigen). At least 10^9 lymphocytes guarantee a quick adaptive immune response. There are many different types of lymphocytes, but only three main classes all of which have surface receptors specific for the antigen. B cells (lymphocyte B) secrete antibodies and are therefore the most important lymphocytes for the analytical chemist. Lymphocytes that produce antibodies against molecules of the host system are eliminated by a process called tolerance. A failure of the tolerance system leads to autoimmune disease. On the first exposure to a foreign molecule, the immune response is relatively slow. On the second exposure, lymphocytes produced during the first exposure recognise the antigen early and can react in a fast and strong immune reaction (antibody production). This mechanism is known as immunological memory.

2.7.3.2 Antibody Structure

Antibodies are a large family of glycoproteins. They can be classified in five classes, IgG, IgM, IgA, IgE and IgD. Immunoglobin G (IgG) is the most abundant immunoglobin species in serum and also the most commonly used antibody in sensor applications. Structural features are easiest explained using the IgG molecule that consists of one Y shaped unit (Figure 1). An IgG molecule can be described as consisting of four polypeptide chains, two identical heavy (H) chains and two identical light (L) chains (Figure. 1) [52]. The length of the two chains is 450 amino acids for the H-chain (~55,000 Dalton) and 212 amino acids for the L-chain (~25,000 Dalton). The two identical H-chains are connected via disulphide bridges. The connection between the L-chain and the H-chain consists also of disulphide bonds. Since all these bonds connect two chains they are named interchain disulphide bridges. Both chains L and H also have interchain disulphide bridges. The globular structure of the protein, that is responsible for the name immunoglobulin, is a result of these interchain bonds. The H-chain is divided into four sub domains and the L-chain into two sub domains. These sub domains are classified according to the variability of their amino acid sequence, into constant (C) and variable (V) regions. The sub domains of the H-chain are three C regions, C_H1, C_H2, C_H3 and one V region, V_H. The two sub domains of the L-chain are one C region and one C region C_L and one V region V_L. The base of the Y shape is called the fragment that crystallises (Fc) and is formed by the association of the two C_H2 and the two C_H3 domains. Each arm of the Y shape is called a Fab (fragment containing antigen binding site) and is formed by association of C_H1 with C_L and V_H with V_L. The small domain between C_H1 and C_H2 is called the hinge region and allows lateral and rotational movement of the Fab fragments. Furthermore, the

terminal amino group of the amino acid sequence is allocated at the end of the Fab fragment, whereas the Fc fragment contains the terminal carboxyl group. For the antibody antigen interaction however, most of the IgG fragments are of minor importance. The binding site (paratrope) is located within the V_H and V_L domains and each arm contains one binding site. In the variable regions, amino acid sequences can vary from antibody to antibody and allow the specific adaptation to certain antigens. The exact regions within these variable regions that have very high amino acid variability are called hypervariable regions, also known as complimentary determining regions (CDRs). Three CDRs are integrated into the L-chain and three into the H-chain, resulting in six CDRs for each arm. The variability created by the CDRs of each Fab fragment allows the creation of 10^8 different binding sites.

The other sub domains are also of functional importance. C_H1 binds complementary C4b fragment, C_H2 contains carbohydrate binding sites and C_H3 domains are responsible for the interaction with the rest of the immune system. The H-chain is different for different immunoglobulin. IgG has a γ-chain, IgM a μ-chain, IgE a ε-chain and IgD a δ-chain. Differences in the chains result in subclasses such as IgG_1, IgG_{2a}, IgG_{2b} and IgG_3. All these different IgG subclasses mainly differ in the Fc fragment, and they appear and function in different stages of the immune response.

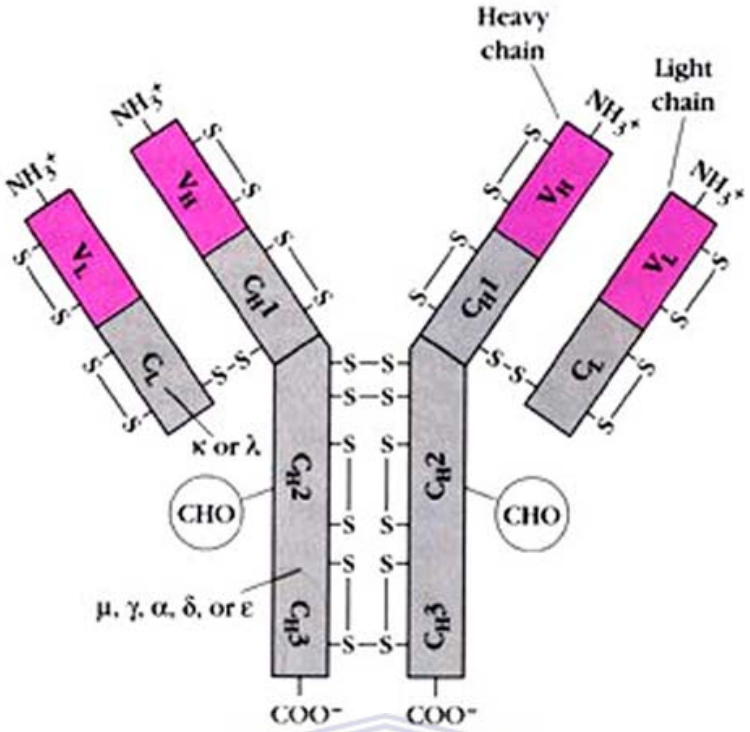

Figure 1. Important attributes of an antibody.

2.7.3.3 Antibody Antigen Interaction-Affinity

The binding of antigens to antibodies is mediated by non-covalent bonds, and is thus a reversible reaction. That is, one can write an equilibrium equation of the type:

[Ag] + [Ab] ⟷ **[AgAb]** (2)

Where, **[AgAb]** represents the concentration of the antigen-antibody complex. The type of bonds that hold the antigen and antibody together in this complex are generally; ionic bonds, hydrogen bonds, hydrophobic interactions, and van der Waals forces. These bonds are formed between the side chains of amino acids that make up the antigen-binding site of the antibody and the antigen molecule. Both, antibody and antigen can undergo substantial conformational changes upon interaction, but they may also stay unchanged depending on the

specific antibody antigen pair. The binding of antigen to antibody can be described by an equilibrium constant that indicates the strength of the interaction. In general antibodies bind with very high affinity to antigens, and K_a (association constant) values in the range of 10^9 or greater are fairly common. The equilibrium of their interaction (Eq 2) can be described with the affinity constant K_A (Eq 3). Ab represents antibody and Ag antigen.

$$\mathbf{Ab + Ab \leftrightarrow Ab\text{-}Ag} \qquad \textbf{(3)}$$

$$K_A = \frac{[Ab-Ag]}{[Ab].[Ag]} \qquad \textbf{(4)}$$

What distinguishes the reaction is typically how long they stay attached before dissociating, which is influenced by the reverse rate constant. This can range over several orders of magnitude, and is mostly influenced by the number and types of bonds that are formed between the antigen and antibody. High affinity complexes are also much more stable. Affinity constants range from 10^5 to 10^{12} M^{-1}.These high affinities are achieved by the tailored binding sites of the epitopes. The loss of one hydrogen bond in an interaction can result in 1,000 fold decreased affinity. Whereas the affinity constant for a monoclonal antibody can be determined, K_A for polyclonal serum is more difficult to determine. Polyclonal antibodies represent a mixture of antibodies, specific for the antigen, whereas monoclonal antibodies consist of identical immunoglobulin molecules. The specifications of immunosensors are determined to a large extent by the affinity of their components. High affinity results in sensitive sensors, but too high affinities might result in virtually irreversible sensors.

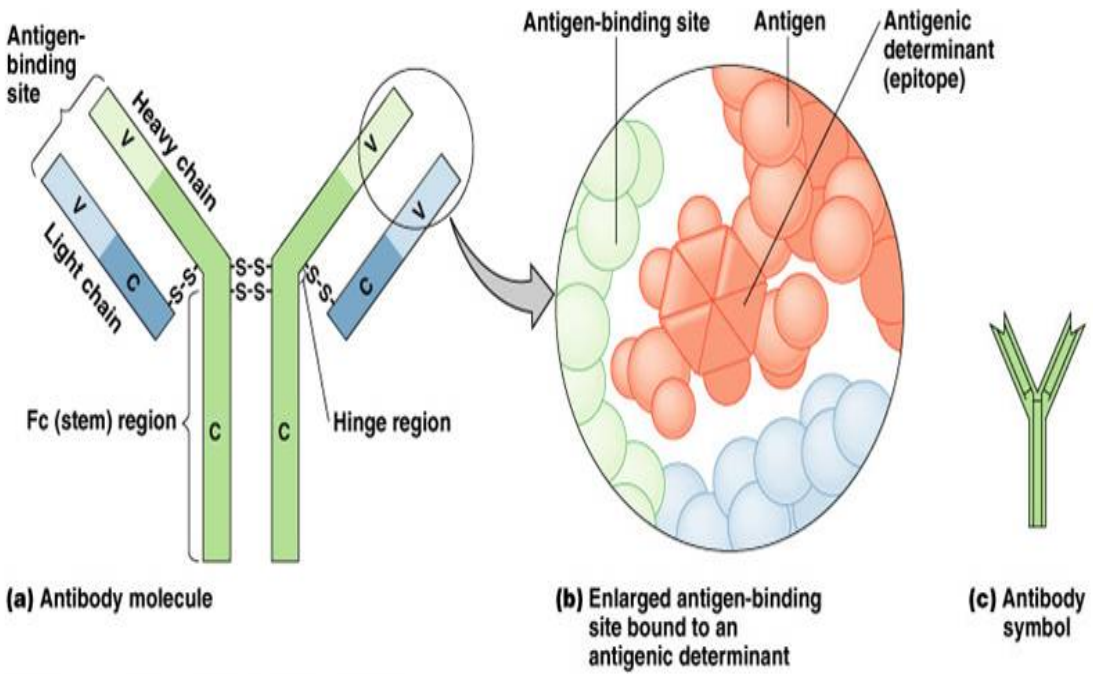

Scheme 8: Antibody Antigen Interaction-Affinity

2.7.3.4 Immobilization methods of biomolecules

The immobilization of the biological element onto the transducer is very important for the biosensor performance [46]. The optimal immobilization method would yield a biomolecule immobilized on the surface of a transducer, retaining its full activity with long-term stability regarding its function and immobilization. Furthermore, the biomolecule should be fully accessible for substrate, analyte, co-reactant, antigen, antibody or oligonucleotide. The transducer should be unaffected by the immobilization step. Many immobilization methods can fulfil a number of these requirements, but they also have disadvantages. Therefore, the immobilization method has to be chosen and adapted for the particular bio element, transducer, matrix and other assay requirements. The most common immobilization methods used for biosensors can be divided into physical and chemical methods. Physical methods

include adsorption entrapment, encapsulation and confining. Chemical methods are cross linking and covalent immobilization. Cross-linking is mostly carried out to improve the stability of physical methods.

2.8.1 Physical Adsorption

Physical adsorption of biomolecules to solid surfaces is a simple technique [53, 54] Many different surfaces are used for adsorbing biomolecules. These materials include cellulose, collagen, PVC, gold and carbon. Proteins are attached to these surfaces by low energy bonds such as charge-charge interactions, hydrogen bonds, van der Waals forces and hydrophobic interactions. The advantage of adsorption as an immobilization method is its simplicity. Frequently, the surface is only incubated in the protein solution for a certain time and then washed to remove excess protein. However, the stability of the protein layer is generally poor and can be affected by many factors, such as pH, ionic strength or temperature. To improve the stability of the adsorbed molecules, they are sometimes cross-linked with bifunctional reagents such as glutaraldehyde. This results in an adsorbed network rather than adsorbed molecules. Unfortunately, the process of cross-linking can deactivate the biomolecules to some extent.

Other techniques passively adsorb proteins, such as protein A or protein G, on the transducer surface resulting in oriented immobilization of antibodies. These proteins are specific for the specific Fc region of certain antibodies and allow the Fab fragments to freely interact with the antigen. Passive adsorption is often used in disposable sensors and ELISAs, where the protein layer is not reused and extended stability is not required to the same extent as in permanent or reusable sensors.

2.8.2 Entrapment

The biological element can be entrapped in a three dimensional polymeric lattice. This is normally achieved by forming a networked polymer gel around the biomolecules. Starch gels, nafion, silicate and polyacrylamide gels are frequently used. The network can be formed by polymerizing a three dimensional structure or by cross-linking two-dimensional polymer strands. Polymerization is also carried out electrochemically. The gel can also be formed with a technique called co-reticulation. A mixture of excess of inactive protein, such as BSA, and the active biomolecules are cross-linked. The resulting network is a gel, formed by the cross-linked inactive protein with the active biomolecules trapped and cross-linked inactive protein with the active biomolecule trapped and cross-linked in the gel. The biological element is homogenously entrapped in the gel but is often only accessible for small molecules. On the other hand, the irregular (heterogeneous) structure of the gel might cause leakage of the biomolecules from less densely polymerized regions. Cross-linking of the molecules might overcome the problem and retain more biomolecules in the gel, but the bifunctional cross-linkers might also deactivate the biological elements.

Gel entrapment is a popular immobilization method for whole cells, but not for antibodies or antigens. Whole cells are retained very well in the gel due to their size and their analytes and substrates are mostly small molecules. In immunogenic reactions, however, mainly large molecules are involved and as such cannot move freely through the gel. Another form of entrapment is the incorporation of the biological element in the electrode matrix. Enzymes can also be incorporated in composite elements. A mixture of graphite particles, enzymes and plasticiser (water insoluble liquid or solid) forms the electrode. Direct incorporation of

biomolecules is also possible when electrodes are screen printed. Carbon ink, for example, is mixed with an enzyme and printed onto a solid support. After drying, the enzyme is permanently entrapped in the electrode.

2.8.3 Encapsulation and Confining

Encapsulation and confining as an immobilization method is mainly used for enzymes. A simple system that was employed in early biosensors is the retention of enzymes on transducers, such as electrodes, by semi-permeable membranes, such as dialysis membranes. Substrates and products can cross this barrier, but the enzyme cannot. Biomolecules can also be confined in microcapsules of either semi-permeable materials or liposomes. However, even when the enzymes are immobilized in the microcapsules, association with the transducer is often difficult.

2.8.4 Covalent Binding

This method involves the formation of covalent bonds. Functional chemical groups belonging to amino acid residues on the surface of the enzyme not essential for activity, may be attached covalently to chemically activated supports (glasses, cellulose or synthetic polymers).The amino groups involved in covalent bond are of lysine or argirine, the carboxyl group of aspartic and glutamic acid, the hydroxyl group of serine and threonine, the sulfydril group of cysteine [55].

Many support materials are available to form covalent bonds. This reflects the fact that no ideal support exists and respective advantages and disadvantages must be taken into account when considering possible procedures for a given enzyme immobilization. Although several factors influence the selection of a particular support, research work has shown that

hydrophilicity is the main factor for maintaining enzyme activity [56]. Polysaccharide hydrophilic gel polymers are popular support materials for immobilization: the sugar residues in these polymers contain hydroxyl groups as ideal functional groups for chemical activation, in order to provide covalent bond formation and to create hydrophilic environment in the support by means of hydrogen bonds. Other popular supports for enzyme immobilization are porous glasses and silica. Porous glasses are also durable and resistant to solvent distortion, even though less hydrophilic than polysaccharides. There are many reaction procedures for coupling an enzyme and a support in a covalent bond. However most reaction fall into four categories:

1. Formation of an iso-urea linkage
2. Formation of a di-azo linkage
3. Formation of a peptide bond
4. An alkylation reaction

It is important to choose a method that will not inactivate the redox site of the enzyme. An enzyme employing a COOH group at its active site will require a reaction that involves an amino group for the covalent bonding with the support. Before the enzyme is added in a coupling reaction, functional groups onto the support should be activated, normally to render them electrophilic, by a specific reagent. It is also possible to chemically modify the normal functional groups in order to produce a range of derivatives containing different functional groups and to extend the possibility of immobilization methods (e.g. cellulose derivatives).

2.8 .5 Cross-linking

This procedure is support-free and involves joining the receptor to each other to form a large, three-dimensional complex structure. Crosslinking or co-crosslinking can be achieved by chemical or physical methods [57]. Chemical method normally involves covalent bond formation between the enzyme by means of bi- or multifunctional reagent, such as glutaraldehyde and toluene di-isocyanides. Both albumin and gelatine has been proved as good molecular spacers to minimise the close proximity problems that can be caused by crosslinking a single enzyme.

Physical crosslinking of cells by flocculation is well known in biotechnology industry and does lead to high cell densities. Flocculating agents, such as polyamines, poly-ethyleneimine, Polystyrene sulfonates, phosphates, have been extensively used and well characterised.

Crosslinking is rarely used alone ass technique of immobilization, because the absence of mechanical properties and poor stability are severe limitations for biosensor development.

This one is often used to enhance other methods of immobilization, normally in order to reduce cell leakage in other systems.

2.8.6 Practical considerations

In biosensing systems with the best response and performance criteria, receptors are commonly immobilised either alone or mixed with other proteins such as bovine serum albumin, as co-crosslinker agent, either directly on the transducer surface, or on a polymer covering it. In the latter case, pre-activated organic membranes can be used directly for the biomolecule immobilization without further chemical modification of the membrane.

Covalent attachment, cross-linking procedures or a combination of both are more complicated than the simple entrapment ones, but are useful in cases where sensor is so small that the appropriate membrane must be fabricated directly on the transducer, in order to obtain more stable and reproducible activities. Furthermore, the biosensor long term stability is largely improved with the combination of two different methods, because the enzyme is both strongly bonded to the support and cross-linked (sometimes also co-cross linked) in a three dimensional lattice.

2.9 Conductive electroactive Polymers

2.9.1 Polypyrrole utilized as platform in electrochemical immunosensors

In 1991 John et al. described a method for incorporation of antibodies in polypyrrole layers. Polypyrrole electrodes were prepared by galvanostatically electropolymerizing pyrrole from an aqueous solution containing anti-human serum albumin (anti-HSA) on a polished Pt electrode. With CV it was shown that HSA does interact with these sensing layers, while no response is obtained with polypyrrole without incorporated antibodies. This method was extended by Sadik and Wallace, who were able to detect the interaction of HSA inflow-injection analysis (FIA) using PAD. This method has also been used for the detection on "non-bioactive" polymers. These polymers have been prepared from an aqueous solution containing 0.2 M pyrrole monomer and 0.1 M p-toluene sulphate. The responses observed are dependent on the nature of the polymer, the nature of the electrolyte/ cation as well as on the electrolyte concentration and pH, which suggested that these factors can be used to modify the selectivity.

Polypyrrole is a conducting polymer. Its charge depends on the applied potential. Prior literature findings have shown that polypyrrole acts as an insulator at negative potentials [58]. This means that by pulsing the potential between 0.4 and 0.0 V, the polymer is alternately positively as dopant anions are expelled into the solution phase, leaving the polymer in its neutral, non-conductive state. When an antibody is incorporated, the antigen is able to bind to the positively charged polymer (that is, at *E*= 0.4 V). When the potential is sufficiently negative, e.g. at -0.6 V, a kinetically controlled electrode process becomes dominant. At positive potentials, the PPy changes electrochemically to its conductive state, thus allowing the diffusion of the anions (dopant) into the film. This anionic uptake is responsible for the polymer exhibiting its desirable electrochemical properties. At 0.0V the polymer with incorporated antibodies has a net negative charge and positive ions from the solution compensate this charge and push aside the antigen. At 0.4V these positive ions either leave the polymer, or their positive charge is neutralized by the anions in the buffer. During binding of antigen, the characteristics of the electrode are different, which results in a different current response, depending on the concentration of antigen in the sample. The resulting positive current difference can be explained by a combination of a decrease in capacitance and an increase in resistance of the electrode.

Bioaffinity sensors based on conducting polymers have been reviewed, and a comparison of different sensing systems suitable for the determination of pesticides, metals and PCBs has been described [59]. Studies on the charge transfer mechanism of an antibody (i.e. antihuman serum albumin) immobilized on a polypyrrole electrode was carried out. The results revealed that the antibody-antigen reaction was responsible for varying the capacitative behavior of the polymer. It was suggested that the interactions between the negatively charged antibody and

the positively charged polypyrrole chain gave rise to the variations in capacitance. Investigations of several antibody immobilization methods (entrapment in a polypyrrole layer and covalent attachment with a silane molecule) were done and a form of impedance spectroscopy (differential impedance spectroscopy) developed to characterize the surface density and antibody-antigen reaction [60].

2.9.1.1 Polypyrrole utilized as electroactive binding layer

Among the conducting polymers, polypyrrole exhibits various physical and chemical phenomena, such as its stability under environmental conditions, thermal stability, biocompatibility and biodegration. PPy protects electrochemical biosensors from interfering with anionic electrochemically active materials, which makes it as one of the most promising for technological and biomedical applications. Conducting polymers have attracted much interest as suitable matrices of biomolecules and can be used to enhance stability, speed, and sensitivity and hence are finding increasing use in medical diagnoses [1]. Based on the latter, Polypyrrole is finding ever increasing use in diagnostic medical reagents [61]. The electronic properties of polypyrrole enables information about biomolecular events occurring on/in the active polymer to be relayed back to the electronic interface to produce analytical signals. The electronic information relayed back may be due to direct oxidation/reduction of the analyte or a product from an enzymatic reaction involving the analyte. In cases where no electroactive species are present, the biomolecular interaction of interest may give rise to a change in electronic properties (conductivity, capacitance) of the polymer and the electrochemical switching properties of the polymer [62].

Another advantage offered by polypyrrole is that the electrochemical synthesis allows the direct deposition of the polymer on the electrode surface, while simultaneously trapping the protein molecules [63] It is thus possible to control the spatial distribution of the immobilized enzymes, the film thickness and modulate the enzyme activity by changing the state of the polymer. Conducting polymers have the ability to efficiently transfer electric charge produced by the biochemical reaction to electronic circuit [64]

2.9.2 Effect of film thickness on cation permselectivity at overoxidized polypyrrole film

The number of studies devoted to the use of modified electrodes has received tremendous attention in recent years [65]. The main reasons to modify electrodes are to improve selectivity and sensitivity of electrodes with modifiers. Previous investigations have shown that the main advantages of polypyrrole films lies in the ability to modify the polymer with different counterions, making them more suitable for the detection of a range of analytes [66]. Polypyrrole undergoes overoxidation at positive potentials and/or at more alkaline media. This transformation is accomplished by a loss of conjugation, electronic conductivity and dedoping with a net electronegative character imparted to the polymer film. Hence, the small doping anions ejected from the OvoxPpy film, creates a porous structure on the electrode. The OvoxPpy film improves selectivity, cation permselective behavior and the efficiency of OvoxPpy in suppressing interfering electroactive species and avoiding electrode fouling.

The high permselectivity of overoxidized polypyrrole films allows analytes to reach the surface easily. According to previous literature findings, it has been shown that overoxidized PPy films (thickness of 0.1 μm) have excellent cation permselectivity. Hence, the thinner the thickness of the overoxidized PPy film, the shorter the response time and a higher sensitivity can be achieved. The permeability of films is expressed by the following equation:

$$P_m = \alpha D_m / \delta_m = D_{app} / \delta_m \qquad (5)$$

Where the P_m (cm/s) is the film permeability, α is the membrane partition coefficient, D_m (cm^2/s) is the diffusion coefficient within the film, D_{app} (cm^2/s) is the apparent diffusion coefficient in the film, and δ_m (cm) is the film thickness. According to eq.5, the permeability of the film increases as δ_m **decreases**. High permeability will allow analyte to reach the surface easily; hence a fast response time and a higher sensitivity can be achieved.

2.9.3 Polypyrrole utilized in label-free impedimetric immunosensors

Prior literature findings have shown that polypyrrole acts as an insulator at negative potentials [67]. This means that dopant anions are expelled into the solution phase, leaving the polymer in its neutral, non-conductive state. When the potential is sufficiently negative, e.g. at -0.6 V, a kinetically controlled electrode process becomes dominant. At positive potentials, the PPy changes electrochemically to its conductive state, thus allowing the diffusion of the anions (dopant) into the film. This anionic uptake is responsible for the polymer exhibiting its desirable electrochemical properties.

A label free and reagentless immunosensor based on direct incorporation of antibodies into conducting polymer films at the surface of the screen-printed electrode (SPE) using an AC impedimetric response electrochemical interrogation was reported by Grant et al., 2005. They indicated that the real component of the impedimetric response acts as a dominant component of AC impedimetric response of anti BSA loaded conducting polypyrrole (PPy)

film on its exposure to the different concentration of BSA. BSA could be detected with a linear response from 0 to 1.136 x 10^{-6} M. The nature of the observed Faradaic current arose due to antibody-antigen interaction. Gooding et al., 2004 fabricated a glassy carbon electrode modified with anti-rabbit IgG antibody entrapped in an electrodeposited polypyrrole membrane for label free amperometric detection of IgG antigen in flow injection system. Lillie et al., 2001 fabricated a simple immunosensor format by polymerizing pyrrole loaded with avidin or antibody to luteinizing hormone (LH) on a gold inter-digitized electrode and demonstrated that impedance spectroscopy can be used to detect LH between 1 and 800 IU/L^{-} . No separation of bound and unbound species was necessary as is the case with conventional immunoassays. An impedimetric immunosensor for the antibiotic ciprofloxacin was fabricated by Garifallou et al., 2007. Polyaniline was electrodeposited onto the sensors and then utilized to immobilize a biotinylated antibody for ciprofloxacin using classical avidin-biotin interactions. Electrodes containing the antibodies were exposed to solutions of the antigen and interrogated using AC impedance protocol. The faradaic component of the impedance of the electrodes was found to increase with increasing concentration of antigen.

CHAPTER 3

3.0 Experimental Methods of Investigation

3.1 Introduction

This chapter consists of the following:

• Materials: Information on all the materials used.

• Research design: A general overview of all the sequential steps taken in other to accomplish the aim of the study.

• Methodology: A more detailed presentation of the instrumental and experimental techniques.

3.2 Materials

Pyrrole obtained from Aldrich purified by distillation and kept in a refrigerator before use. Tissue transglutaminase (tTG) antigen from guine pig liver, anti-transglutaminase antibody produced in goat, anti-human IgG and anti-human IgA peroxidase conjugated antibodies, Bovine serum albumin and doubly distilled water were used to prepare all solutions.

3.3 Buffers and solutions

Buffer 1: Phosphate buffer produced from 0.05 M Sodium dihydrogen orthophosphate (NaH_2PO_4) and 0.05 M Disodium hydrogen orthophosphate (Na_2HPO_4), with the pH adjusted by mixing of adequate volumes of each solution. Bovine serum albumin (BSA), potassium ferricyanide and potassium ferricyanide [$Fe(CN)_6^{3-/4-}$]**.**

Buffer 2: 0.05 ML^{-1} HEPES (N-(2-Hydroxyethyl)-piperazine-N'-2-ethansulfonic acid), use pH 7.0 for solubilisation of the transglutaminase. **Buffer 3**: 10 mM L^{-1} phosphate, 137 mM L^{-1} NaCl, 0.05% (v/v) Tween 20, pH 7.0 was utilize for the incubation and washing step during the antibody detection procedure.

3.4 Electrode Surface Modification

3.4.1 Preparation and stabilization method for gold colloidal nanoparticles (GNPs)

The first step for the synthesis of GNPs is the reduction of Au (III) involving the use of $HAuCl_4$ in the presence of KCl. This is followed by immobilization of GNPs in oxidized polypyrrole film, in which the Au is used to retain the catalytic bioactivity of the enzyme and facilitate the direct electron transfer between the enzyme and the electrode.

3.4.2 Preparation of tTG|GNP|OvoxPPy||GCE

Prior to modification, the base GCE (GCE: ~ 3 mm in diameter) was polished with 1.0-, 0.3- and 0.05 μm alumina slurry. This was followed by thorough rinsing with doubly-distilled water and subsequently, sonicated in absolute ethanol and doubly-distilled water for approximately 5 min, successively, to remove any adsorbed substances on the surface. Finally, it was air-dried and ready for use.

Polymerization was done by placing the clean GCE into deaerated solution of 0.1 M $LiClO_4$ containing 0.1 M (70 μL) pyrrole, and polymerized at a constant potential of +800 mV (vs.Ag/AgCl) for 120 s, under argon atmosphere. The electrode was transferred into a 0.1 M

NaOH solution and overoxidized at a constant potential of 1.0V for 420 s until the current decrease. The GNP was electrochemically deposited onto the OvoxPpy||GCE by potentiodynamic method, scanning from 0.2 to -1.0 V in 0.5 mM $HAuCl_4$ solution at a scan rate of 50 mV/s for 15 cycles. The modified electrode was denoted as GNP|OvoxPpy||GCE. The modified GCE was characterized by CV and SWV.

After the preparation of the nano-composite platform, 40 µL of transglutaminase solution (0.3 mg mL^{-1} prepared in buffer 1) was immobilized onto the platform and incubated for 2 h at 25 ºC. The tTG antigen solution was then removed by rinsing with buffer 3. Subsequently, the unspecific and residual binding sites was blocking by immobilizing 40 µL of BSA (2 mg mL^{-1} prepared in buffer 2) for 1 h. The electrode is denoted as BSA|tTG|GNP|OvoxPpy||GCE. The modified electrode was now ready for use as Immunosensor for the detection of anti-transglutaminase antibodies. The detection of anti-transglutaminase antibodies was accomplished by incubating the Immunosensor with standard solutions of anti-transglutaminase antibodies (from goat) for 1h at 25 ºC. After incubation, the Immunosensor was transferred to a equimolar solution of Fe $(CN)_6^{3-/4-}$ redox probe and analyzed by electrochemical impedance spectroscopy.

Scheme 9. Schematic illustration of the stepwise immunosensor fabrication process

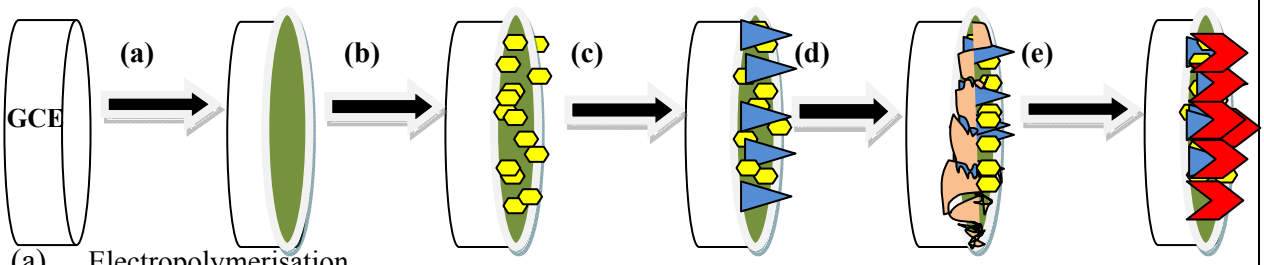

(a) Electropolymerisation

(b) Electrochemical reduction : Ppy-$HAuCl_4$ composite

(c) Transglutaminase antigen immobilization

(d) BSA blocking of residual and unspecific binding sites

(e) Anti-transglutaminase incubation

Note: Binding of protein is possible by electrostatic interaction with the surface modified negatively charged OvoxPpy film and the GNP's.

3.4.3 Antibody preparation

Antibody solution is prepared by diluting the required concentration of antibody in 1000 µL of PBS pH 7.4. A range of concentrations was utilized (1:200-1:4000), since CD is noted at very low anti-tTG concentrations.

3.4.4 Choice of scan rate

Prior to immobilization of tTG antigen, a freshly prepared GNP|OvoxPpy-composite electrode was exposed to Voltammetric measurements as described in section 3.4.2 above except that the potential was held constant at +200 to -1000 mV while varying the scan rates.

3.4.5 Choice of potential window for EIS

A freshly prepared GNP|OvoxPpy modified electrode was used in this part. The cell set up was as described in section 3.4.2. Electrochemical impedance spectroscopy were performed on the GNP|OvoxPpy modified electrode in 1ml Fe $(CN)_6^{3-/4-}$ and analyzed at different potentials (0-400 mV).

3.4.6 Stability studies

The storage stability of the immunosensor was also investigated over a period of 5 days. When the electrode was not in use it was suspended above 0.1 M phosphate buffer at 4 ºC, the R_{ct} changes was then monitored by running the EIS over the 5 days.

3.4.7 Electrochemical Characterization of Antigen-GNP|OvoxPpy||GCE

All electrochemical experiments were carried out and recorded with a computer interface to a BAS/50W integrated automated electrochemical workstation (Bioanalytical Systems Lafayette, IN, USA). Cyclic voltammetry are carried out in a 10 mL electrochemical cell, with Ag/AgCl (3 M NaCl type) and platinum wire as reference and auxiliary electrodes respectively and glassy carbon electrode are utilized as working electrode. The impedance of the modified electrode are measured with Zahner (IM 6 ex), impedance measurement unit. Impedance measurements performed at the frequency range of 0.5-1000 Hz, with a sinusoidal potential modulation of ± 10 mV superimposed on the applied dc potential. Impedance measurements are performed in buffer (10 mM L^{-1} phosphate, pH 7.0) including 2.5 mM L^{-1} $Fe(CN)_6^{3-/4-}$ at a bias potential of 0.200 V. Using a conventional three-electrode cell with a volume of 1 ml. The impedance data are fitted to an equivalent circuit using the implemented THALES software.

3.4.8. Scanning Electron microscopy (SEM)

The procedure for preparation of the GNP|OvoxPpy-composite materials for SEM analysis was similar to that described in **Section.3.4.2**. However, screen printed carbon electrodes were used as the working electrode instead of the GCE. Pre-treatment of the screen printed electrodes involved repeated potential scanning in 0.2 M H_2SO_4 in the potential range of -1200 mV to +1500 mV at a scan rate of 100 mV/s, until reproducible voltammograms were obtained. After electrodeposition, the GNP|OvoxPpy modified electrodes were thoroughly rinsed with deionised water and kept in sealed Petri dish containers in readiness for SEM analysis. The SEM analysis was performed on a JEOL JSM-7500F Scanning Electron Microscope.

Methodology

3.5 Analytical techniques

3.5.1 Electrochemical impedance spectroscopy (EIS) characterization

The development of hand held devices for point of care measurements is a promising alternative to existing laboratory based immunochemical assays. In most immunosensors, the antibody is immobilized onto a conductive support, and the electrical properties of the interface are modified when the antibody reacts with the antigen of interest.

Characterizing the immobilization of the antibody along with its stability/activity and interaction with the antigen are important steps in optimising the analytical performance (i.e. selectivity, stability, sensitivity, response time etc) of the immunosensor. The formation of an antigen-antibody complex on a conductive support alters the impedance features of the interface, and impedance spectroscopy has been used to study the antigen-antibody molecular recognition event by measuring the resistive and/or capacitive change that accompanies this reaction.

Studies by Corry et al. 2003 showed that EIS is a powerful method for predicting the surface activity of an immunosensor. The impact of immobilization on the antibody-antigen binding event was studied, and it revealed that covalent attachment of an antibody to the electrode surface is needed for a successful impedance-based immunosensor.

3.5.2 Electrochemical Impedance measuring parameters

Electrochemical impedance spectroscopy (EIS) provides detailed information on interfacial kinetics as it relates to capacitance and electron transfer resistance changes. Label free immunosensors that use EIS signals are sometimes called impedimetric biosensors. In EIS, impedance *Z* is given as a ratio of the applied voltage to its current response. There is usually a phase shift j in between the voltage (or current) applied and current (or voltage) response. If the interfacial electrochemistry involves electroactive specie, it is termed faradaic impedance and charge transfer resistance, R_{ct}, is mostly used as the reporting impedance element. On the other hand, if the interfacial electrochemistry is in the absence of electroactive specie, it is called non faradaic impedance. EIS measurement can be performed in either of these two ways (i) faradaic measurement of the charge transfer resistance R_{ct} over a wide frequency range and (ii) non faradaic measurement of impedance or capacitance at single frequency.

Electrical impedance is defined as a ratio of an incremental change in voltage to the resulting change in current. Either and AC test voltage or AC test current is imposed while the other variable is measured. Mathematically, if the applied voltage is $V_{test} = V_{DC} + V_{AC} \sin(\omega t)$ and the resulting current test is $I_{test} = I_{DC} + I_{AC} \sin(\omega t - \psi)$, then the complex-valued impedance Z has magnitude V_{AC}/I_{AC} and phase ψ. The electrode-solution impedance depends on both the bias conditions (V_{DC}) and the measurement frequency (ω). By exciting with a single frequency, a lock in amplifier can be used to accurately measure the output signal at the same frequency. Voltage excitation is usually employed in EIS because the most troublesome parasitic impedances are in parallel with the measured electrode-solution impedance. In most cases, the measurement process is repeated at different frequencies yielding Z.

In impedance biosensors, the applied voltage should be quite small, usually ≥ 10 mV or less for 2 main reasons: (i) the current-voltage relationship is often linear for only small pertubations [68]. (ii) To avoid disturbing the probe layer. Therefore, impedance is frequently defined in the context of the linear current voltage relationship. Furthermore, since typical covalent bond energies are in the order of 1-3 eV, it is very important to prevent disturbance of the probe layer especially since applied voltages can exert a disruptive force on the charged molecules. This second consideration also applies to DC bias voltages across the electrode-solution interface. However, accurate EIS measurements do not damage the biomolecular probe layer, an important advantage over conventional voltammetry or amperometry where more extreme voltages are applied.

Variations of standard impedance spectroscopy include using multiple excitation frequencies simultaneously, exciting with noise [69], and exciting with a voltage step (which contains frequency components) [70]. Such approaches could decrease the time required per measurement and avoid complications due to the fact that impedance is poorly defined especially when the experimental system is likely to undergo localised changes in the course of the electrochemical measurement and data acquisition.

3.5.2.1 Electrodes

At minimum two electrodes are needed to measure electrolyte-solution impedance, and usually three are used. The current is measured at the working electrode and is bio functionalized with the probe. In order to establish a desired voltage between the working electrode and solution, electrical contact must be made with the solution using a reference electrode and/or counter electrode. A reference electrode maintains a fixed, reproducible

electrical potential between the metal contact and the solution allowing a known voltage to be applied. A simple piece of silver wire-a pseudo reference [71] can sometimes suffice. A counter electrode supplies current to the solution to maintain the desired electrode-solution voltage, usually in electronic feedback with the reference electrode monitoring the solution voltage.

3.5.2.2 Instrumentation in Electrochemical Impedance spectroscopy

A potentiostat imposes a desired command voltage between the solution and working electrode while simultaneously measuring the current flowing between them. EIS analyzers are potentiostats designed especially for measuring AC impedance and have typical frequency ranges of 10 MHz-100 kHz. Computer control is ubiquitous for both potentiostats and EIS analyzers. Digital post processing is commonly employed to amplify the signal and to eliminate background noise.

3.5.2.3 Faradaic vs. Non-Faradaic

Faradaic EIS requires the addition of a redox-active species and DC bias condition such that it is not depleted. In contrast, no additional reagent is required for non-Faradaic impedance spectroscopy, rendering non-Faradaic schemes somewhat more amenable to point of care applications. The term capacitive biosensor usually designates a sensor based on a non-Faradaic scheme, usually measured at a single frequency.

3.5.2.4 Data Fitting

The measured impedance data can be used to extract equivalent values of resistances and capacitances if a circuit model is assumed a priori, this can be achieved despite the absence of a fixed unique model or even a one-to-one correspondence between circuit elements and the

underlying physical processes [72]. Figure 2.1 shows typical circuit models, and Figures 2.2 and 2.3 shows examples of impedance data. It is not always necessary to fit data to a model, and even the best models of the electrode-solution interface do not always perfectly fit experimental data without relevant fitting parameters. Sometimes the raw impedance is fit to a model and changes in model elements are reported as the sensor output. Alternatively, the impedance at a particular frequency is used. Depending on the values of the respective model circuit parameters, data at a particular frequency can contain information about various circuit elements or be influenced by a single element.

3.5.2.5 Circuit Models

Figure 2 shows the two most common models used to fit impedance biosensor data, depending on whether a Faradaic or non-Faradaic measurement is made. The solution resistance R_{sol} arises from the finite conductance of the ions in bulk solution, and thus generally not affected by binding. The capacitance between the metal electrode and ions in solution C_{surf} can be modelled as a series combination of the surface modification capacitance and the double layer capacitance. The component due to surface modification depends on the thickness and dielectric constant of the probe layer. It can be thought as a parallel plate capacitor, whose capacitance is given by $C = \varepsilon_r \, \varepsilon_o \frac{A}{t}$ where $\varepsilon_r\varepsilon_o$ is the relative dielectric constant, A is the electrode area and t is the insulator thickness. The capacitance C_{surf} is often modelled by a constant phase element instead of a pure capacitance. In parallel with this capacitance there is a resistive path modelled by R_{leak} for non Faradaic sensors or the series combination of Z_w and R_{ct} for Faradaic sensors. For an ideal insulator or when no redox species is present, R_{leak} is theoretically infinite. The Warburg impedance (Z_w), is only of physical significance in Faradaic EIS, represents the delay arising from diffusion of the

electroactive species to the electrode. It is only appreciable at low frequencies, is affected by convection (and thus may be invalid for experimental time scales), and has a phase shift of 45°.The charge transfer resistance (R_{ct}) is a manifestation of two effects (1) the energy potential associated with the oxidation or reduction event at the electrode (i.e. the overpotential) and (2) the energy barrier of the redox species reaching the electrode due to electrostatic repulsion or steric hindrance. The two circuit elements most commonly used as indication of affinity binding are C_{surf} for non-Faradaic biosensors and R_{ct} for Faradaic ones [69].

3.5.2.6 Constant Phase Element

The impedance of solid electrodes usually deviates from purely capacitative behaviour, this is empirically modelled as a constant phase element (CPE).The complex impedance of a CPE is given by $1/J\omega A)^m$ where A is analogous to a capacitance, ω is the frequency expressed in rad/s and $0.5 < m < 1$ ($m = 1$ corresponds to a capacitor and $m = 0.5$ corresponds to a Warburg element; m for C_{surf} modelling is typically 0.85 and 0.98). This introduces a sub 90° phase shift, or equivalently a frequency-dependent resistor in addition to a pure capacitor.

CPE behaviour can be explained mathematically by dispersion in local capacitance values. Microscopic chemical inhomogenities, ion adsorption and inhomogeneous current distribution contribute to CPE behaviour [73 74] . Since solid electrodes can be expected to have a certain amount of intrinsic CPE behaviour, modelling the electrode-solution interface as purely capacitative is often an over simplification which can reduce the quality of the data fit.

3.5.2.7 Double Layer Capacitance

When an electrode is polarized relative to the solution, it attracts ions of opposite charge. This tendency is countered by the randomizing thermal motion of the ions, but results in a local build-up of excess ions of opposite charge. Thus, any electric field arising at the electrode or within ionic solution decays exponentially because the excess ions screen the field. The characteristic length of this decay or Debye length is proportional to the square root of ion concentration [69]. This effect creates a capacitance called double layer capacitance or diffuse layer capacitance. Ions adsorbed at bare electrodes also increase the capacitance in accordance with the Gouy-Chapman-Stern. The double layer capacitance is voltage-dependent because increasing the electrode voltage attracts the diffuse ion layer, increasing capacitance [69]. If an insulator (e.g. an insulating probe layer) covers the electrode, forming a capacitance, the double layer capacitance appears in series with it. In impedimetric biosensors, the ionic double layer usually plays a minor in the overall measured impedance since it is so large relative to series capacitance of the probe layer for non Faradaic sensors and because the parallel path through Z_w and R_{ct} dominates at relevant frequencies for Faradaic sensors.

(a)

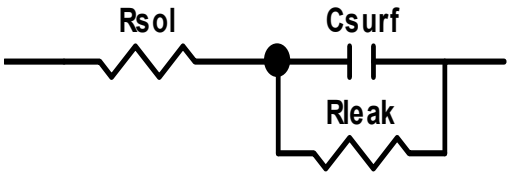

(b)

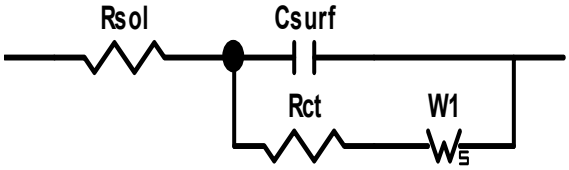

(c)

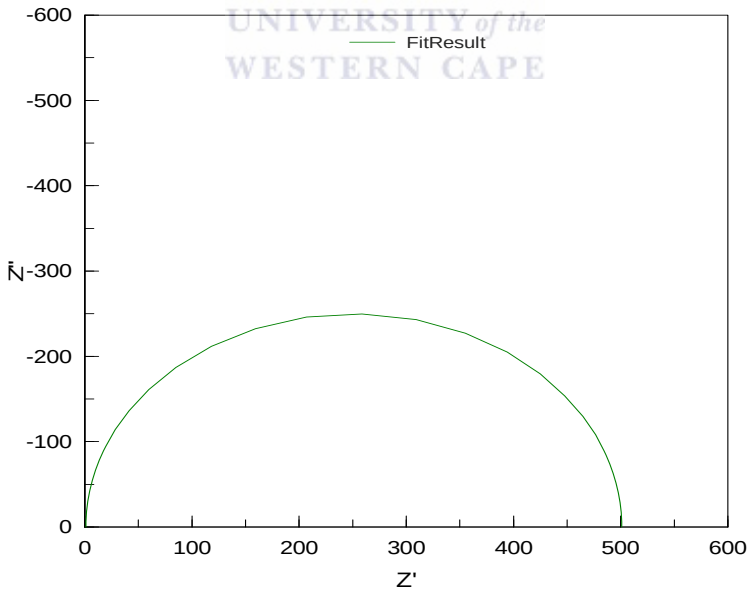

(d)

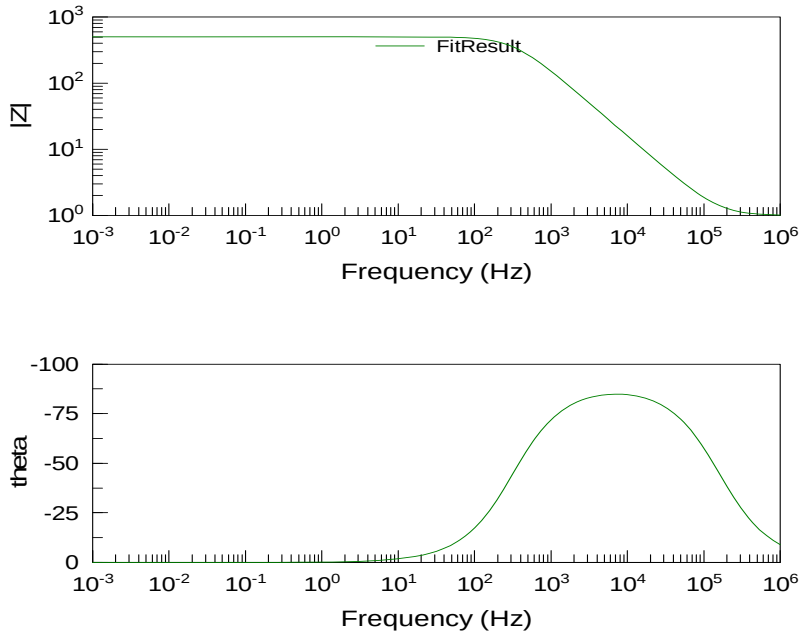

Figure 2. Common circuit models for (**a**) non-Faradaic and (**b**) Faradaic interfaces. **(c)** non-Faradaic impedance data in Nyquist representation (**d**) Faradaic impedance data in magnitude/phase (bode plot) representation.

3.6 Cyclic Voltammetry

Cyclic voltammetry is the most widely used electrochemical technique for studying the nature of electrochemical reactions in detail [69]. During the cyclic voltammetry experiment the potential is scanned from the starting potential (Ei) to the final potential (Ef) and back to Ei and the resulting current is measured. During the electrochemical measurement the solution is kept stationary. The data obtained is represented as a current-potential plot known as a cyclic voltammogram shown in Fig 3.

In Fig 3, the forward scan represents the oxidation of reductant (Red) to it oxidized (Ox) species, which on the backward scan is reduced. The electrochemical change in species from the reductant to the oxidized species results in the loss of electrons and this process is observed in cyclic voltammogram as a peak, referred to as an anodic peak. The reverse scan, the oxidized species undergo reduction to its reduced species resulting in the gain of electrons and a peak is observed in the cyclic voltammogram, referred to as cathodic peak. The information obtained from the cyclic voltammogram includes the anodic ($E_{p,a}$) and cathodic ($E_{p,c}$) peak potentials and the anodic ($I_{p,a}$) and cathodic ($I_{p,c}$) peak currents. Cyclic voltammetric processes may be reversible, irreversible or quasi-reversible [75].

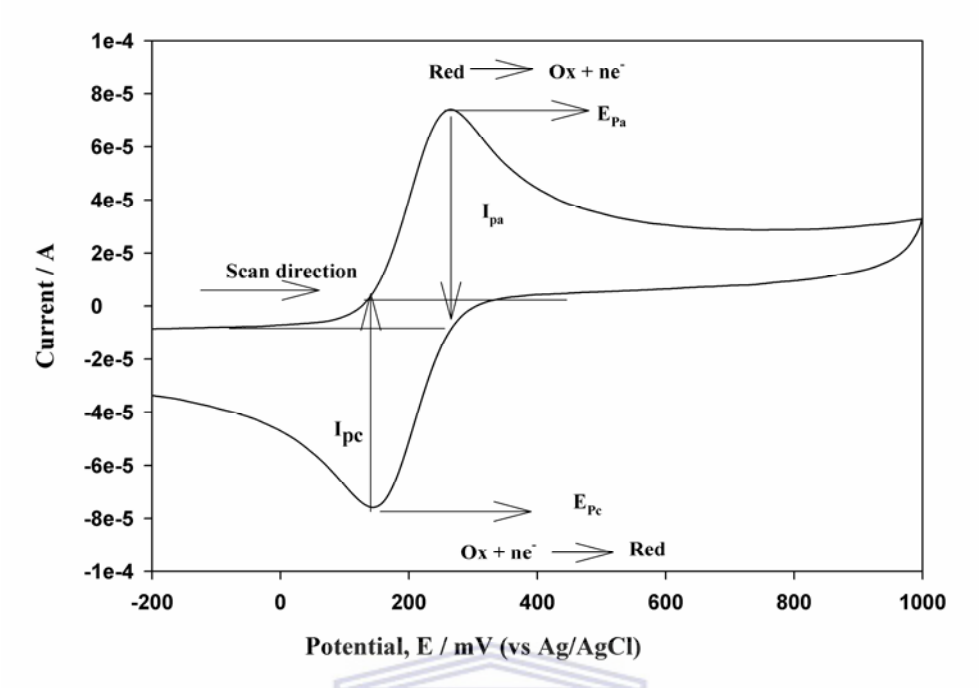

Figure 3 Typical cyclic voltammogram for a reversible process.

(i) *Reversible process*: occurs when an electroactive species in solution is oxidized (or reduced) in a forward scan and reduced (or oxidized) in the backward scan. This type of system is in equilibrium throughout the potential scan.

(ii) *Irreversible process* is the process where the reaction goes one-way, the most

common is when only a single oxidation or reduction peak with a weak or no reverse peak [75] is observed. Irreversible processes are a result of slow electron transfer or chemical reactions at the surface of the working electrode. A large peak potential separation (>200 mV) also indicates an irreversible reaction, if there is a return peak.

(iii) *Quasi-reversible process* exhibits behavior which lies between the reversible and irreversible processes. Differences between the three cyclic voltammetric processes are summarized in table 1.

Table 1: Summary of parameters for diagnosis of reversible, irreversible and quasi reversible cyclic voltammetric processes.

Parameter	Reversible	Quasi-reversible	Irreversible
$\mathbf{E_p}$	Independent of υ	Shift with υ	Shift cathodically by 0.03/αn V for a 10-fold increase in υ
$\mathbf{E_{p,a} - E_{p,c}}$	~ 0.059/n V at 25 ^{o} C	May approach 60/n at low υ but increases as υ increases.	No return peak or >200 mV
$\mathbf{I_{p,a}/I_{p,c}}$	Equals 1 and independent of υ	Equals 1 only if $\alpha = 0.5$	Usually no current on the reverse scan
$\mathbf{I_p/\upsilon^{1/2}}$	Constant	Constant	Constant

α = transfer coefficient, υ= scan rate (V/s), V = volts.

3.7 Square wave voltammetry

Square wave voltammetry (SWV) has proved to be a suitable to investigate redox reactions with overlapping waves. The excitation signal in SWV consists of a symmetrical square wave pulse of amplitude superimposed on staircase wave form of step height ΔE. The forward pulse coincides with the staircase step.

The net current (i_{net}) is obtained by taking the difference between the forward and the reverse currents (i_{fwd}-i_{rev}) and is centered on the redox potential. In SWV, the peak height is directly

proportional to the concentration of the electroactive species and direct detection limit as low as 10^{-8} M is possible.

SWV is associated with some advantages over cyclic voltammetry. These advantages include excellent sensitivity and rejection of back ground currents. The scanning speed in SWV is also high. The high speed coupled with computer control and signal averaging allows for experiments to be performed repetitively and increases the signal to noise ratio. SWV is also applied to study electrode kinetics with regard to preceding, following or catalytic homogeneous chemical reactions and determination of species at trace levels.

3.8 Scanning electron microscopy (SEM)

A scanning electron microscope (SEM) is a powerful microscope that uses electrons rather than light to form an image of objects such as fractured metal components, foreign particles and residues, polymers, electronic components and biological samples among others. It uses a focused beam of high energy electrons to generate a variety of signals at the surface of solid specimens. The signal derive from electron-sample interaction and reveal information about the sample including external morphology (surface texture), chemical composition, crystalline structure and orientation of materials making up the sample. The advantages associated with SEM include among others its ability to perform analyses of selected point locations on the sample. Areas ranging from approximately 1 cm to 5 microns can also be imaged in a scanning mode using conventional SEM techniques (magnification ranging from 20X to approximately 30,000X and a spatial resolution of 50 to 100 nm).

CHAPTER 4

4.0 RESULTS AND DISCUSSION 1

4.1 Preparation of overoxidized polypyrrole (OvoxPpy) on glassy carbon electrode

Polypyrrole was electrochemically prepared from an aqueous solution of 0.15 M distilled pyrrole (the monomer) by potentiostatic method in 0.1 M $LiClO_4^-$ supporting electrolyte. Polymerization was done at a constant potential of +800 mV (vs Ag/AgCl) for 120 s, under argon atmosphere. Electrochemical polymerization of pyrrole proceeds through the coupling of cation radical monomer of the pyrrole. In the oxidized form, the cationic product contains a staggered, conjugated π-electron network that can be balanced with dopant ions such as ClO_4^- .Chemical bonding in conducting polymers provide one unpaired, π-electron per carbon atom in the backbone of the polymer [76] Carbon atoms are in sp^2pz configuration in the π-bonding and orbital's of successive carbon atoms overlap; providing delocalization of electrons along the backbone of the polymer [77]. During polymerization, cations from electrolyte are expected to exhibit electrostatic repulsion forces with radical cations of pyrrole monomers. This repulsion forces largely depend on the charge of cations. Lithium ions having larger effective charge due to localization of charge in a small size readily expel the radical cations of pyrrole monomers out of the region where precipitation of the intermediate occurs. Hence, coupling chance of radical cations with each other becomes smaller due to repulsion forces between the lithium ion and radical cations. Generation of radical cations in the region of the base electrode is much larger in the potentiostatic polymerization and it is hard to retain the electrolytic cations because the electrode maintains constantly at a higher positive potential. Thus the current decrease observed from Fig 4 is expected, as it indicates

increase in radical cation concentration as polymer film thickness increases. The applied potential sufficient to oxidize the pyrrole monomers allow for continues mass increase. This indicates that electrochemical growth of polymer is very much dependent on the applied potential.

Polypyrrole undergoes overoxidation at positive potentials, and/or at more alkaline media, which has been regarded as an undesirable degradation process, which leads to the loss of conductivity and dedoping [28]. In aqueous solution, the Ppy overoxidation potential depends on the solution pH. The higher the pH the lower the overoxidation potential. Indeed, Ppy overoxidation process is more effective in basic solution (NaOH) than in NaCl solution. In sodium hydroxide solution, the overoxidation of polypyrrole film proceeds faster than in median pH buffer solutions because hydroxide ions in sodium hydroxide solution act as nucleophilic reactants which are stronger than anionic species present in buffer solutions [30]. Upon completion of the overoxidation procedure, diffusion of anions in the film is hindered by the formation of carbonyl groups on the polymer. The generation of these higher density carbonyl groups, creates favorable conditions for cationic species to be accumulated onto the film through ion-exchange equilibrium process.

During the overoxidation of the polypyrrole (Fig 5), the current was monitored. Figure 5 shows that initially, a large current was passed, which rapidly decreased as the oxidation progressed. The current eventually leveled off and began to equilibrate slightly around one value. This was taken to indicate complete overoxidation. This process took approximately 6 min.

4.2 Electrodeposition of gold nanoparticles on the OvoxPpy||GCE

Gold nanoparticles were electrodeposited from an argon degassed solution of 100 mM KCl, containing 0.5 mM $HAuCl_4$. Electrodeposition was done potentiodynamically, by cycling the potential from +200 to -1000 mV at a scan rate of 50 mV/s for 15 cycles. The gold nanoparticles-modified GCE, denoted as GNP|OvoxPpy||GCE, was then carefully rinsed and dried. The oxidized polypyrrole film was used as a matrix to allow uniform and stable incorporation of GNPs. GNPs are biocompatible and facilitate the direct electron transfer between biomolecules and the electrode.

The current-potential graph for the GNP-deposition is shown in Fig.6.

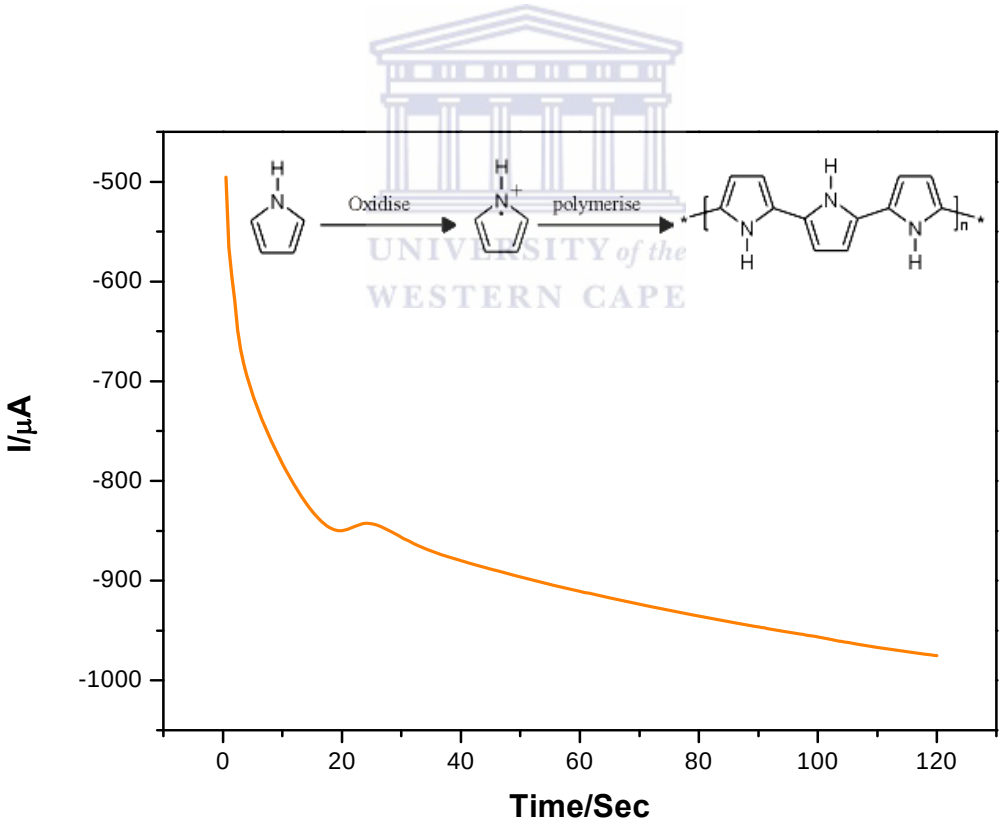

Figure 4. Polymerization process of 0.15 M pyrrole monomer in 0.1 M $LiClO_4^-$ at +800 mV for 120 s

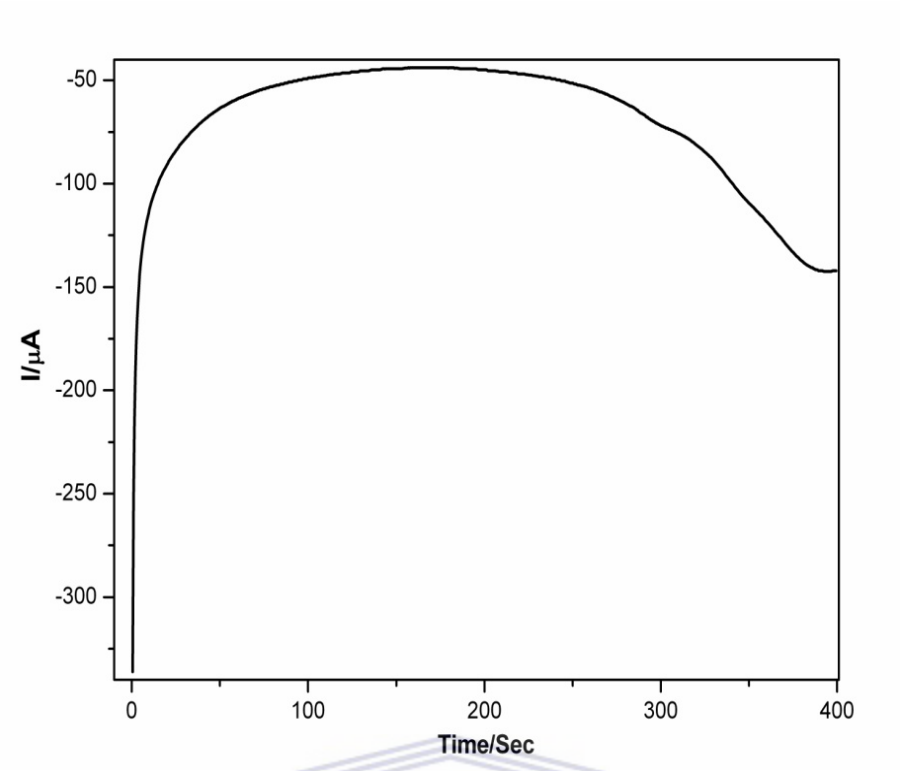

Figure 5. Overoxidation of polypyrrole in 0.1 M NaOH for 400 s

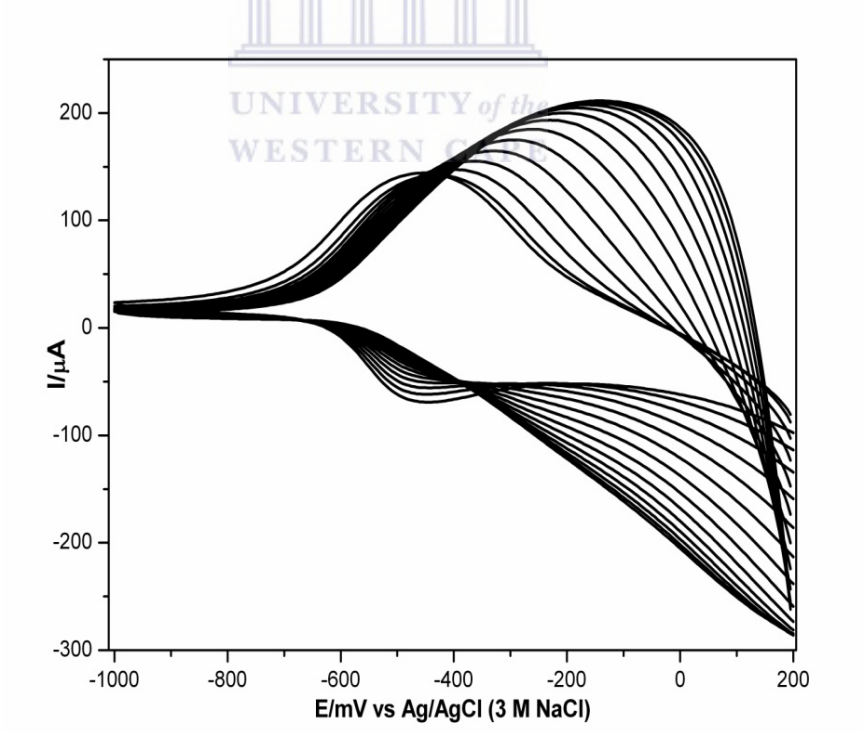

Figure 6. CV of Gold Nanoparticles deposition onto OvoxPpy||GCE

4.3 Morphological characterization of the electrode assembly

Surface morphological characterization of the electrodeposited films during electrode assembly process was conducted by SEM analysis. Figure 7(a) and (b) show the scanning electron micrographs of the Ppy-modified GCE and the OvoxPpy-film, respectively. The micrographs were recorded at a magnification of 30 000, with a scale of 1μm. Figure 7(c) and (d) show the micrographs of electrodeposited gold nanoparticles on the bare glassy carbon electrode and on OvoxPpy||GCE, respectively. These micrographs were also recorded at a magnification of 30 000.

On the bare glassy carbon electrode, shown in figure 7(c), the nanostructures of the electrodeposited gold nanoparticles are hardly observable, scanty and unevenly distribution. Whereas the overoxidized polypyrrole film impregnated with gold nanoparticles exemplifies a more even distribution with more gold deposition. The micrograph is further enlarged as shown in figure 7 (e), taken at a magnification of 80 000 (scale = 200 nm), it is evident that the nanostructures showed very good surface coverage across the overoxidized polypyrrole film, while also exhibiting roughly uniform size, with diameters determined as approximately 100 nm. The good coverage and even distribution of the deposited gold nanoparticles is an expected phenomenon and a likely explanation is that the expelling of the ClO^- dopant ions during overoxidation of the polypyrrole resulted in the creation of nanopores across the OvoxPpy-film which created a suitable matrix for the electrodeposition of the gold nanoparticles. This suggests that the proposed method for formation of OvoxPpy-GNPs composite film can prevent the GNPs from agglomerating. The OvoxPpy-film had a typical "cauliflower-like" structure, constituted by spherical micro-grains (Fig. 7b).

(a)

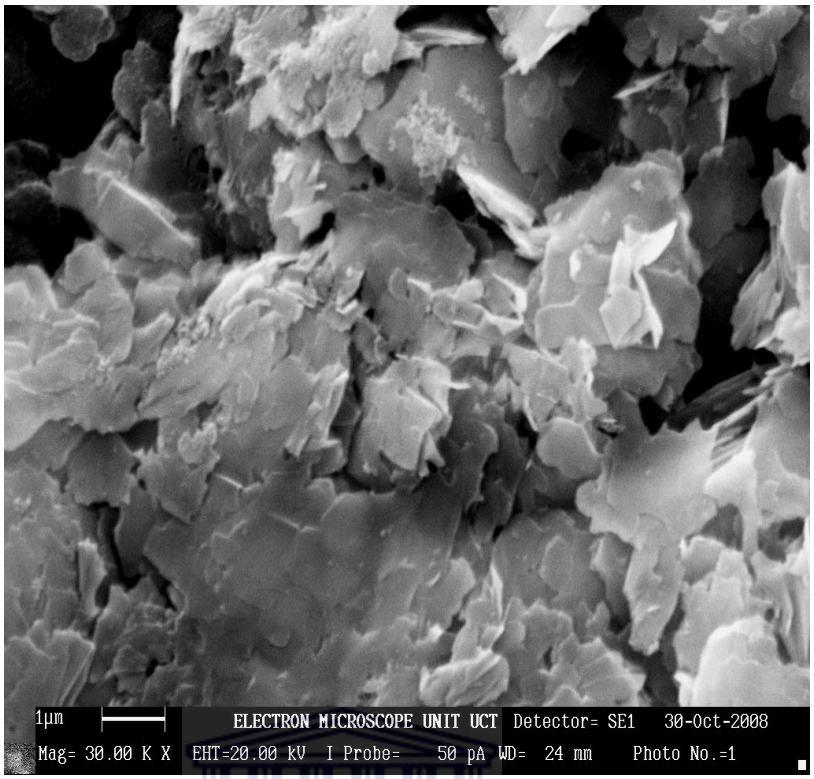

(b)

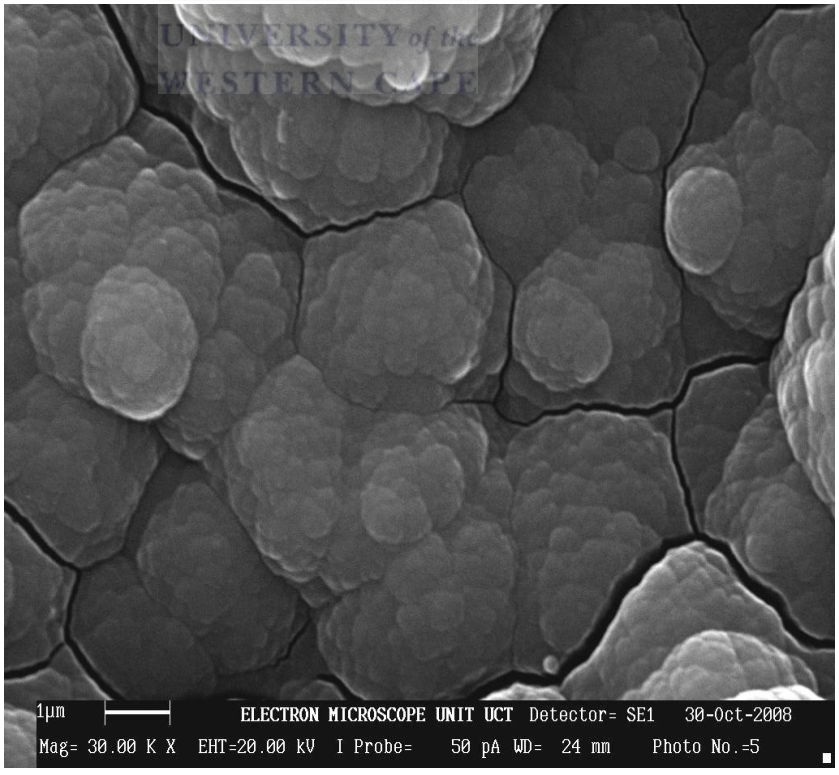

(c)

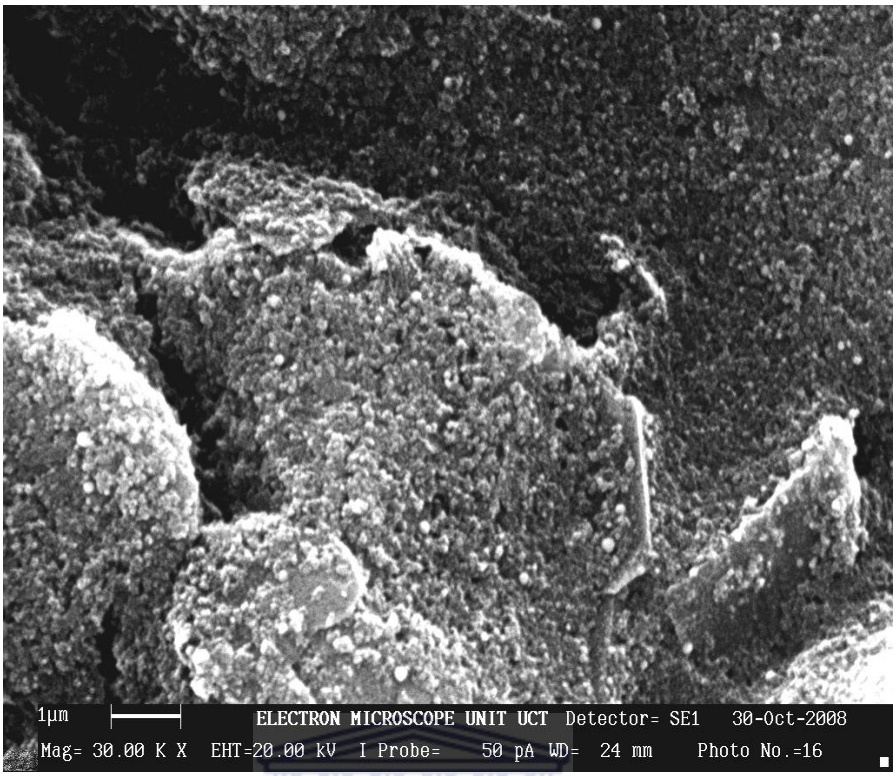

(d)

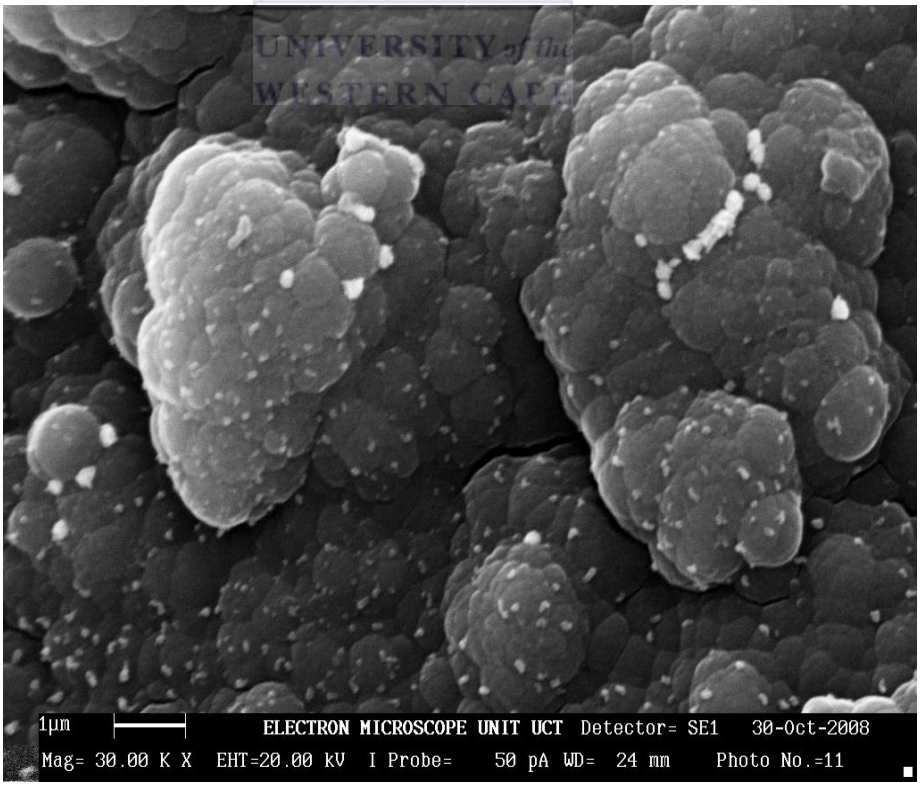

(e)

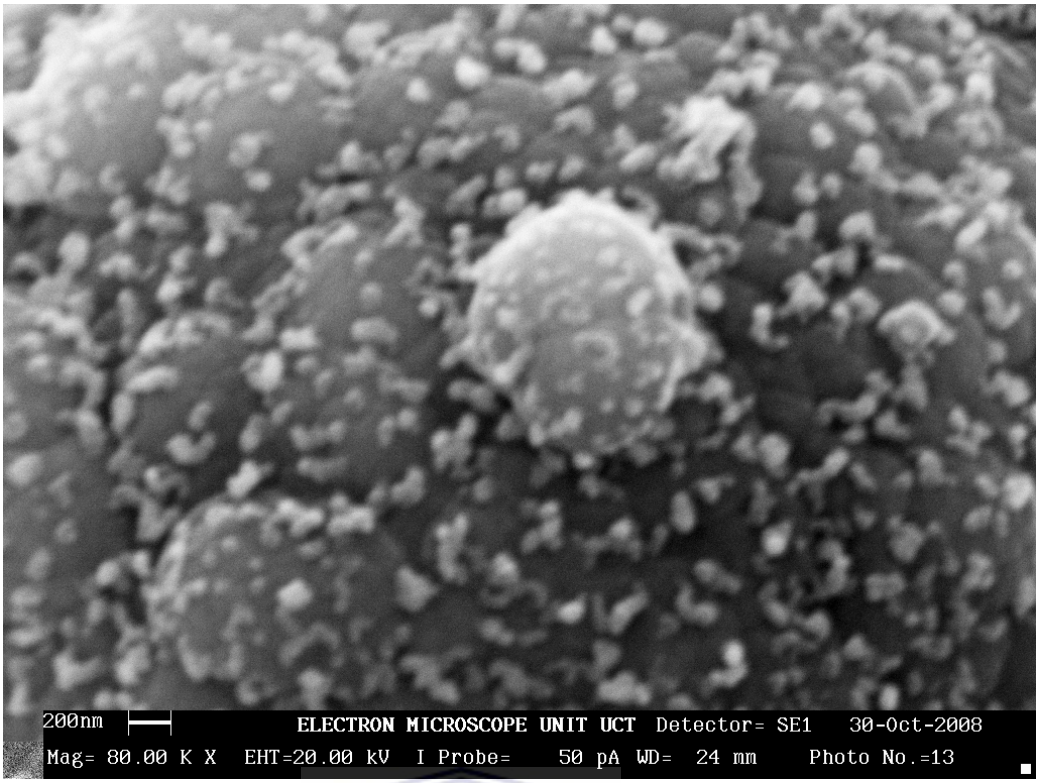

Figure 7(a): SEM of the ClO_4^-doped plainly formed conductive polypyrrole film. **(b):** SEM of the overoxidized polypyrrole-film on the GCE, OvoxPpy||GCE. **(c):** SEM of the gold nanoparticles electrodeposited on the bare glassy carbon electrode, GNP||GCE. **(d):** SEM of the gold nanoparticle|overoxidized polypyrrole composite film, GNP|OvoxPpy||GCE **(e):** SEM micrograph of a selected segment of the gold nanoparticle-overoxized polypyrrole composite.

4.4 Electrochemical characterization of the modified electrode in PBS

Cyclic voltammetry (Fig 8) was used in conjunction with square wave voltammetry (Fig 9) to corroborate the effect of GNP on the OvoxPpy. While the bare GCE (wave c) shows no redox peak, the overoxidized polypyrrole shows a broad oxidation and reduction peak (wave a). The amplified polypyrrole peaks shown in wave b indicates the incorporation of gold nanoparticles into the overoxidized polypyrrole matrix (as shown in SEM image Fig.). These results show that the effective surface area can be greatly enlarged by the incorporated Au-

nanoparticles. In both voltammograms, GNP is seen to amplify the redox currents of the Ppy by about 300 percent! The ΔE values were also smaller; -30 mV for GNP|OvoxPpy and -80 mV for OvoxPpy. The change in potential (ΔE) value is often a measure of the reversibility of a system which also means the speed of electron or charge transfer. In the wise, GNP can be said to speed up the rate at which charges are transferred interfacially at the electrode surface. The unique properties of GNP which has been discussed in Chapter 2 contribute to these changes.

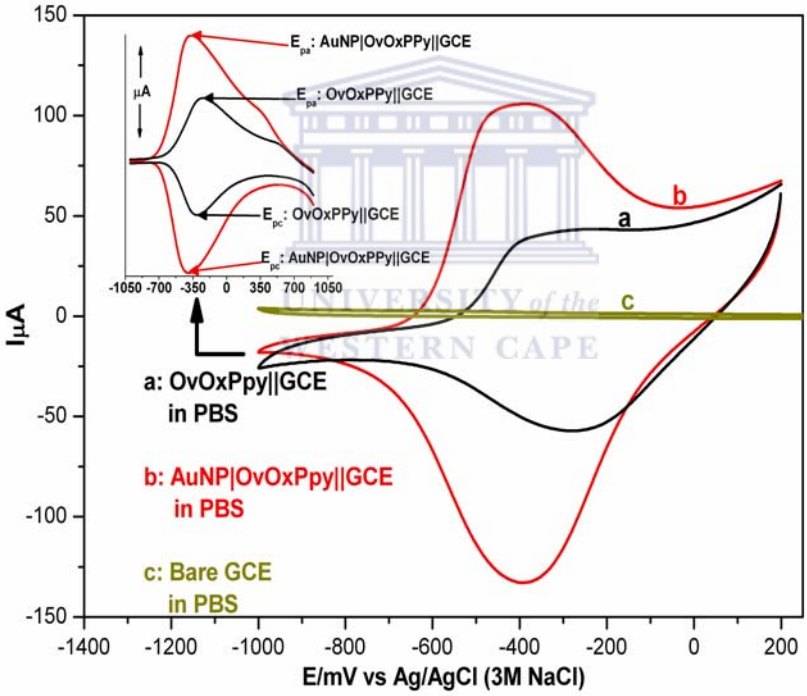

Figure 8: Cyclic voltammograms of the bare glassy carbon electrode (c), the overoxidized polypyrrole film (a) and the gold nanoparticles overoxidized polypyrrole composite film (b). CVs were recorded in argon saturated PBS (pH 7.4) at 70 mV/s. **Inset**: Forward and reverse square waves of the overoxidized polypyrrole film and the gold nanoparticles modified overoxized polypyrrole composite film at 5 Hz frequency.

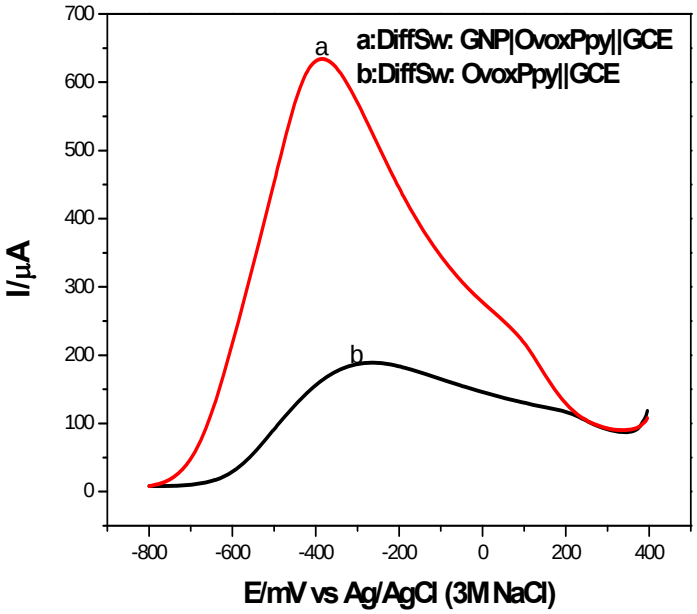

Figure 9. Shows the square wave curves (SW) of GNP|OvoxPpy||GCE (a) and OvoxPpy||GCE (b) in PBS (pH=7.01) at 50 mV/s.

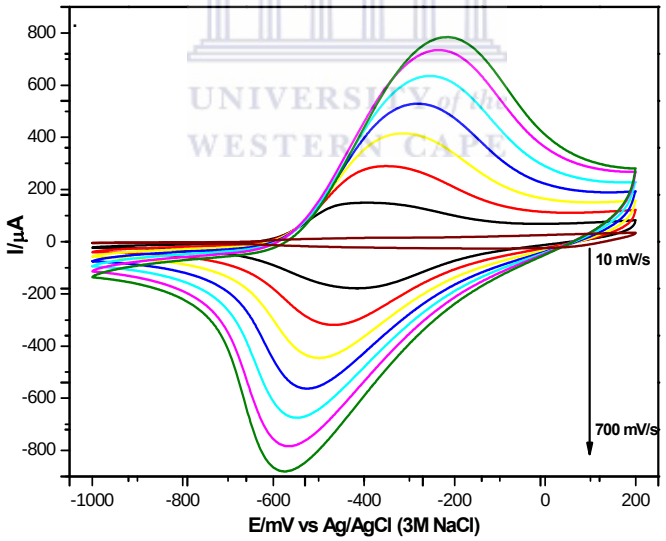

Figure 10. CV of the GNP|OvoxPpy||GCE. Recorded in argon saturated PBS (pH 7.4) at increasing scan rates (10-700 mV/s) versus Ag/AgCl.

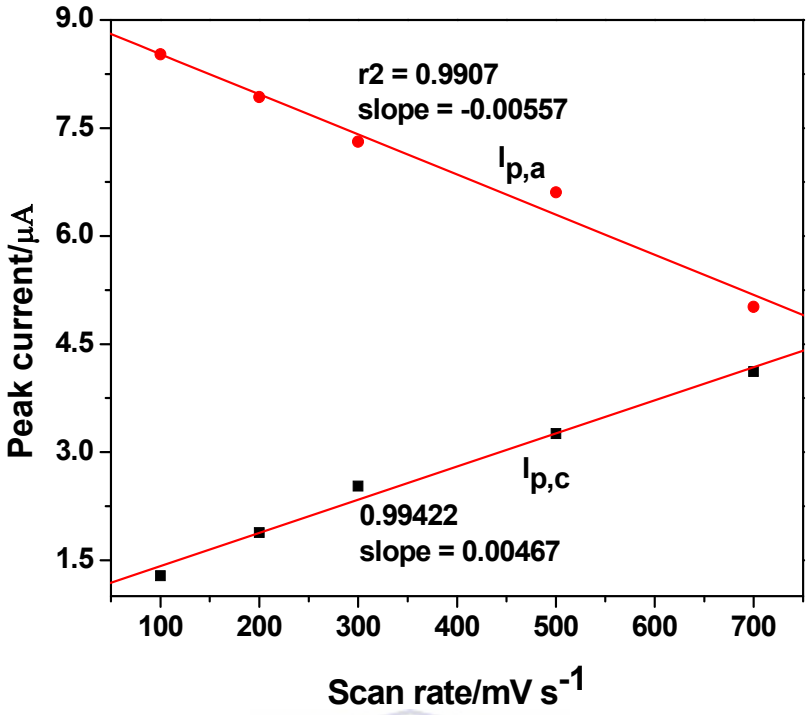

Figure 11. The plot of the dependence of peak currents on scan rate

Voltammetry response of the biosensor to varying scan rate was also studied, the results of which are shown in Fig 10. It is observed that on increase in *v*, the modified electrode showed gradual increase in peak currents as well as a shift in potential resulting in moderate change in peak-to-peak separation with each consecutive scan rate change. Based on the results shown in Fig 10, it may be deduced that the GNP|OvoxPpy composite film was stable and exhibited reversible electrochemistry. The surface concentration, Γ^{*}(mol cm^{-2}), of the adsorbed electroactive species may be estimated from equation 6. [69]:

$$\frac{I_{p,a}}{v} = \frac{n^2 F^2 A\Gamma^*}{4RT} \quad \ldots.(6),$$

Where *n* is the number of electrons transferred, F (96500 C mol^{-1}) is the faraday constant, A (0.071 cm^2) is the area of the glassy carbon electrode, *R* (8.314 J mol^{-1} K^{-1}) is the gas constant and T (K) is the absolute temperature of the system. Therefore, the slope of the linear $I_{p,a}$ vs *v* plot is equal to the right hand side of Equation 5. The anodic and cathodic peak currents show a linear dependence on scan rate. This behavior is in agreement with that of a thin film adsorbed electroactive species undergoing Nernstian reaction. Prior literature studies have shown that the ion exchange behavior of conducting polypyrrole is associated by a one electron transfer process in which the monomers are oxidized by oxidizing agents or catalysts to produce the radical polymer cation [78, 79]. Thus for the one electron transfer process at 25 ^oC, the Γ^* value evaluated from the slope of the anodic slope in Fig.11 is 6.99 x 10^{-7} mol cm^{-2}, and this value lies within the monolayer region.

4.5 Electrochemical characterization of the modified electrode in $Fe(CN)_6^{3-/4-}$ and $Ru(NH_3)_6^{3+}$ redox probes.

$Fe(CN)_6^{3-}$ and $Ru(NH_3)_6^{3+}$ were chosen as electrochemical redox probes to investigate the prepared electrode because of their similar size and fast kinetics on carbon electrodes, however, of opposite charges. The electrochemical response of $Fe(CN)_6^{3-}$ is shown in Fig 12A. The CV curves at the bare GCE shows a redox peak at a middle potential of 0.340 V and peak-to-peak separation (ΔE_p) of 54 mV (curve a). From the CV curves only a small sigmoid wave appears at the OvoxPpy||GCE (curve b). Almost no voltammetric response is

observed at curve b, indicating that the film is negatively charged with a large loss of electroactivity. The negative charge of the layer should be unfavorable for the approaching of ferricyanide anions. This suggests that the film is anionic, which is an advantage as far as its intended application as immobilization layer for tTG antigen, which is a cationic biomolecule is concerned. Furthermore, the CV peak current shows a moderate enhancement (21.9 μA) at the GNP|OvoxPpy||GCE with (ΔE_p) of about 56 mV (curve c). The increase of peak current can be attributed to the increase of effective surface area due to the presence of the Au-nanoparticles. Figure 12B shows the CV response of Ru $(NH_3)_6^{3+}$. In comparison with the CV at the bare GCE (curve a), there is a distinctive difference between the peak currents of 97.2 and 64.8 μA at the OvoxPpy||GCE (curve b) and GNP|OvoxPpy||GCE (curve c), respectively. The response increase at OvoxPpy||GCE could be attributed to the negatively charged OvoxPpy film, which readily attracts more Ru $(NH_3)_6^{3+}$ to the modified electrode surface due to its permselectivity towards cations; thus it also prevents possible interaction of interfering compounds. While electrodeposited GNP's on the porous-OvoxPpy film, significantly enhances the catalytic activity of the composite.

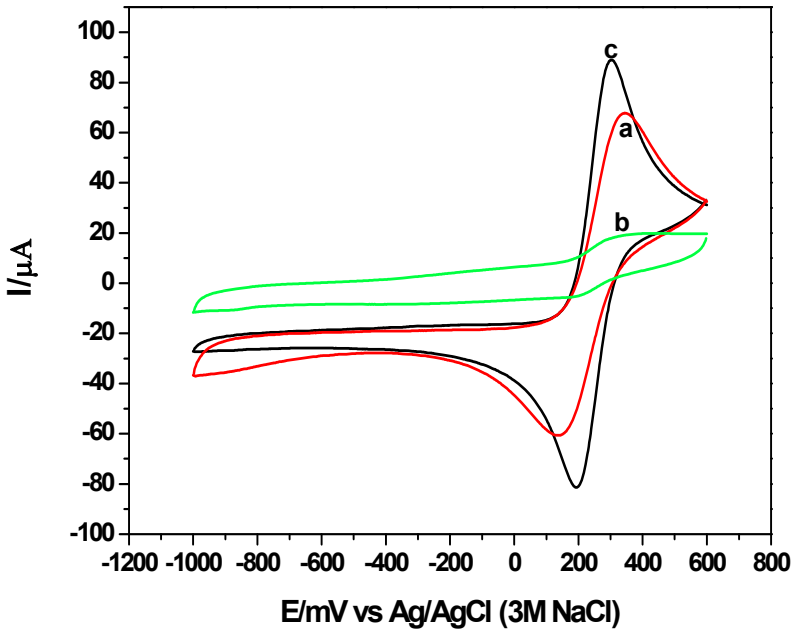

Figure 12 A. Cyclic Voltammogram of 0.001 M Fe $(CN)_6^{3-}$ in 1.0 M KCl at bare (a), OvoxPpy||GCE (b), GNP|OvoxPpy||GCE (c). Scan rate: 50 mV/s

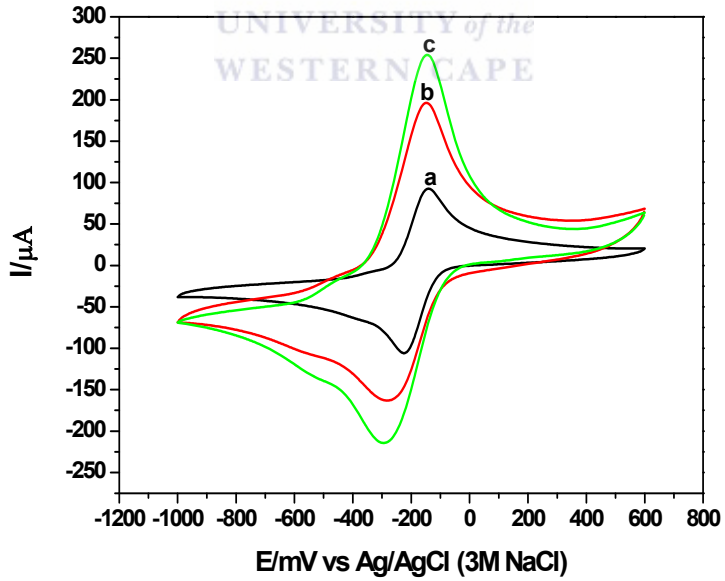

Figure. 12 B. Cyclic Voltammogram of 0.001 M $Ru(NH_3)_6^3$ in 0.1 M PBS (pH 7.0) at bare (a), OvoxPpy||GCE (b), GNP|OvoxPpy||GCE (c). Scan rate: 50 mV/s.

CHAPTER 5

5.0 RESULTS AND DISCUSSION 2

5.1 Choice of potential for EIS

In EIS experiment, the choice of dc potential is crucial for acquisition of the data that most reflect the electroactive behavior of the species under investigation. A redox potential of 200 mV was obtained for Fe $(CN)_6^{3-/4}$ from Fig 12A. Figure 13A, shows the bode plot of the interfacial electron transfer resistance measured over a potential range of 0 and +400 mV (100 mV potential step). This experiment was carried out to corroborate the redox potential obtained from CV. The lowest charge transfer resistance R_{ct} occurred at 200 mV. At this potential, the rate of electron transfer (or flow of current) is optimum and the lowest impedance is expected as seen in Fig 13A. The probe is expected to report best the interfacial changes on the electrode surface at different stages of the immunosensor development at 200 mV.

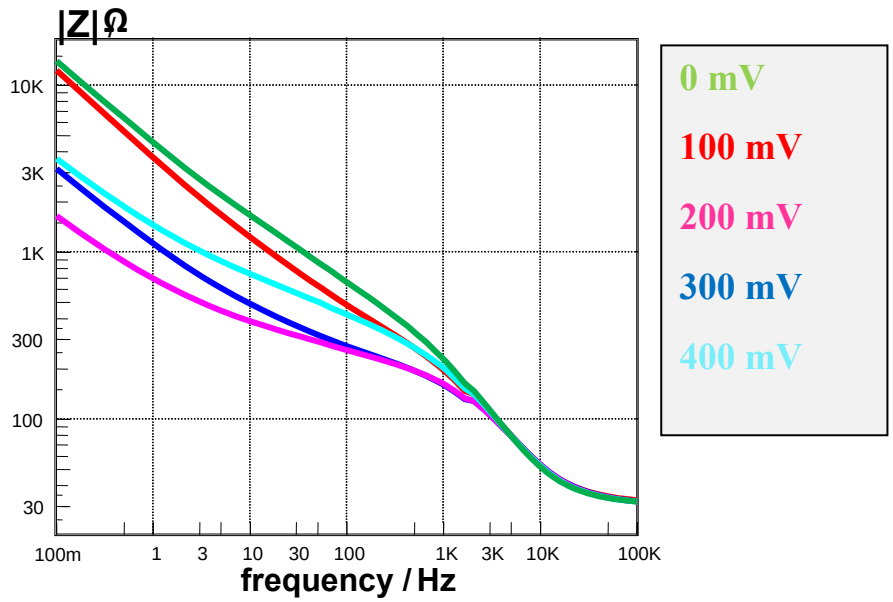

Figure 13A. The bode plot of GNP|OvoxPpy film measured over a potential range of 0 and +400 mV in Fe $(CN)_6^{3-/4-}$ redox probe.

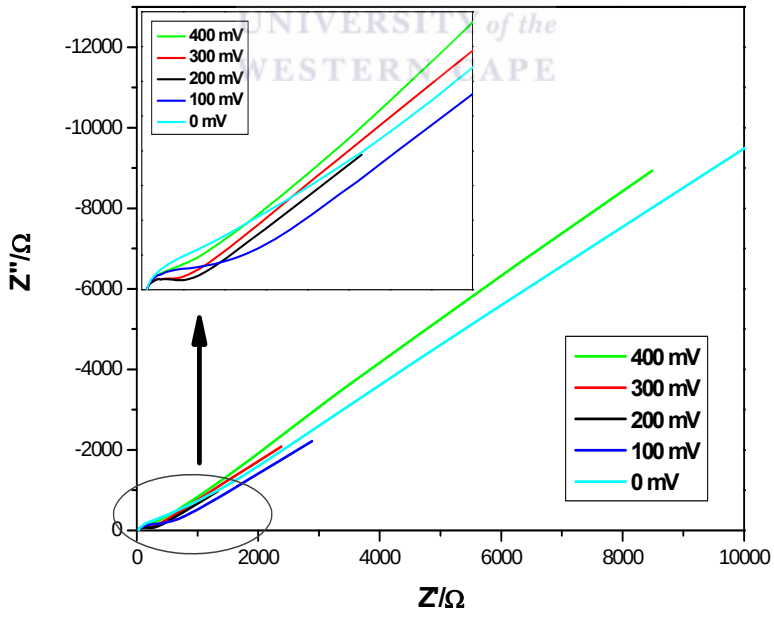

Figure 13B Nyquist plot of electrochemical impedance spectrum at various potentials (0-400 mV).

5.2 Optimization of the experimental parameters

It is well known that the response of the antigen-antibody reaction greatly depends on the time and temperature of incubation, for this reason the effect of temperature and incubation time on the electrochemical behavior of the immunosensor was investigated. As shown in Fig 14A, increasing incubation temperature from 18 °C to 40 ºC, the immunosensor displayed a maximum increase in impedance at 35 ºC with incubated antibody solution. However, the activities of the immunoprotein do not maintain for a long periods of time at this temperature. Therefore, the 25 ºC (room temperature) was selected as the optimum incubation temperature for further experiments. Moreover, because it takes time for the antigen to bind to the modified electrode surface to form the immunocomplex, the effect of incubation time was also investigated. At 25 ºC, the modified working electrode was incubated for 20, 40, 60, 80, 100, 120 and 140 min with Hepes buffer pH 7, containing 0.3 mg/mL tTG. Figure 14B, shows the R_{ct} readily increased within the first 120 min and then tend to stabilize, suggesting an equilibrium state was reached. Therefore, in this study the incubation time of 2 hrs was utilized to insure complete surface coverage of the antigen for immunosensor fabrication.

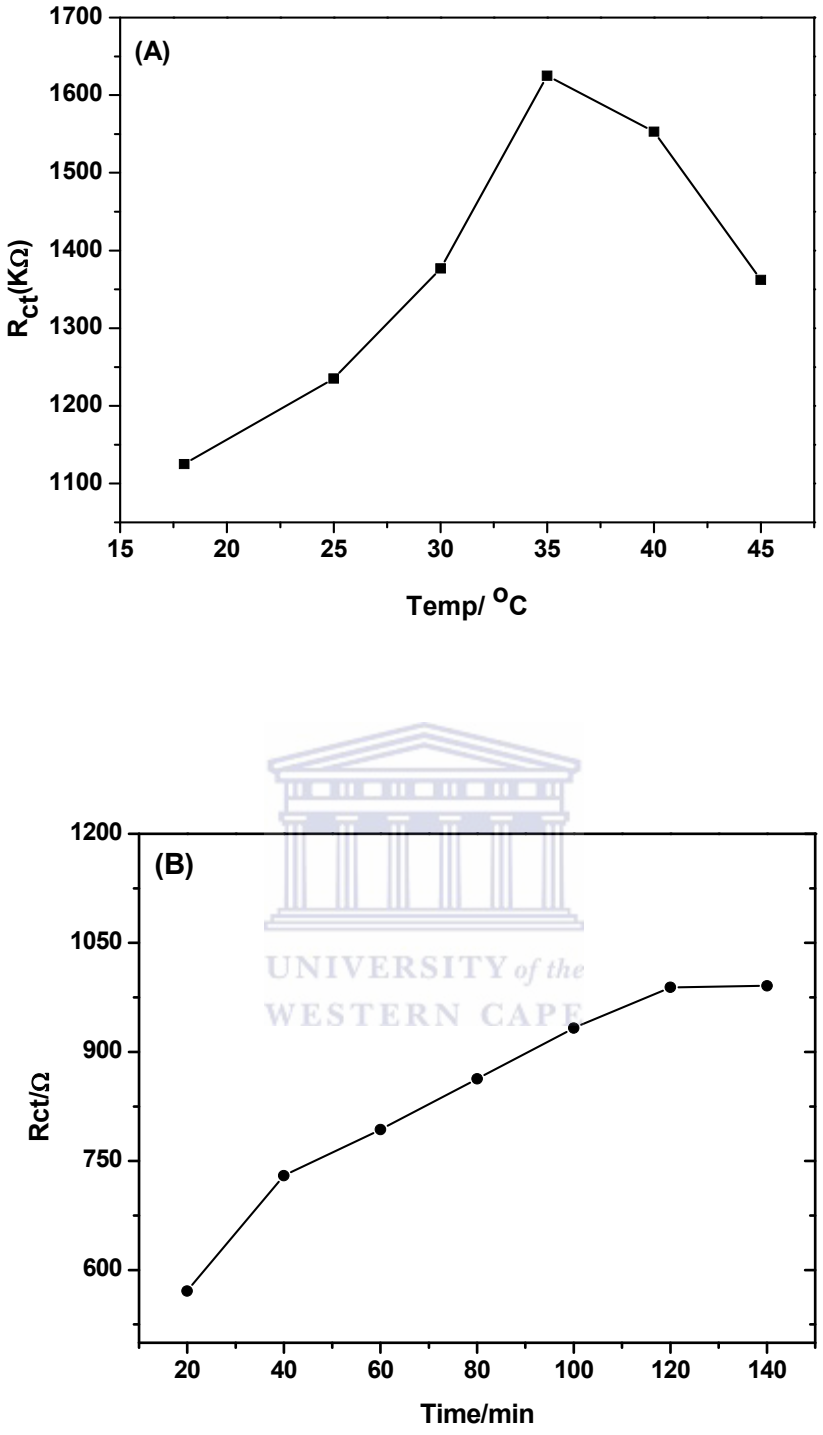

Figure 14. The influence of temperature (A) and time (B) on the response of the immunosensor

5.3 Characterization of the immunosensor with transglutaminase antibody concentrations in Fe $(CN)_6^{3-/4-}$ redox probe.

Figure 15A, shows the impedance spectra recorded after the individual steps of the assay procedure. The collection of impedance data from the glassy carbon electrodes after the different incubation steps in the frequency range from 100 mHz-100 Hz, resulted in an impedance spectrum which includes a semicircle portion at high frequencies corresponding to the electron transfer limited process and the beginning of the linear portion at the low frequencies resulting from the diffusion limited electrochemical process [80]. The increase or decrease in the diameter of the semicircle at high frequencies is associated with the blocking of the electron transfer of the redox probe Fe $(CN)_6^{3-/4-}$ at the interface, due to the adsorption of proteins which are less conducting on the electrode surface. Therefore, binding of the antibody to the immunosensor resulted in significant impedance increase. Table 2 shows the Randles fitting values of the different sensor phases at a single antibody concentration of (1:1000). The value for the element R_{sol} changed only moderately and the capacitance value is slightly decreasing. The capacitance change can be explained by the increase in layer thickness on the electrode surface after each consecutive step of immunosensor fabrication. Furthermore, a clear increase in the R_{ct} value could be detected. Therefore, the R_{ct} element of the Randles equivalent circuit can serve as a sensor parameter: the determination of its value allows the detection and quantification of anti-transglutaminase antibodies in solution. Table 2 also show that at higher frequencies small deviations appear in the absolute impedance, however this is not important for the determination of R_{ct} as sensor parameter, as can also be seen in the Nyquist plot (see Fig. 15A).

For better visualization over the whole frequency range, the measured impedance data were plotted in a Bode diagram, Fig 15B, to show the modulus and phase shift of the impedance. Using the phase angle Bode plot, an estimation of the time constant $\tau = RC$, which can be a kinetics index (ease of transfer of ions across the polymer membrane) of the modified GCE surface in the presence of redox probe $Fe(CN)_6^{3-/4-}$ ion was also carried out. The phase plot at its maximum or peak is characterized by frequency f_ϕ and can be expressed by equation 7, while maximum angle ϕ max is expressed as equation 7 [81]

$$f_\phi = \frac{1}{4\pi RC}\sqrt{1 + \frac{R}{R_S}} \qquad (7)$$

$$\phi = \tan^{-1}\left(\frac{1}{1+\frac{2R_S}{R}}\right) \qquad (8)$$

R and C represent the charge transfer resistance and capacitance, respectively. From $\tau = RC$, equation (7) can be re-written as.

$$\tau = \frac{1}{4\pi f_\phi}\sqrt{1 + \frac{R}{R_S}} \qquad (9)$$

From equation 9, τ is inversely proportional to the frequency which suggest that shift in the maximum frequency of a phase angle plot is indicative of kinetic changes.

Table 3 also shows the calculated τ from the f_{ϕ}. The smaller the value of τ, the faster the kinetics and in this case, the lower the charger transfer resistance. The τ values can also guide in the choice of frequency should one decide to use a narrower frequency range in the same electrolyte for other purposes. Equation 8 justifies the reduction in the maximum phase angle with respect to reduced charge transfer. In summary, as seen in Table 3, the immunosensor has lower R_{ct} and τ values at high frequencies while at lower frequencies, increase in τ can be associated with the blocking of the electron transfer of the redox probe $Fe(CN)_6^{3-/4-}$ at the interface, due to the adsorption of proteins on the electrode surface.

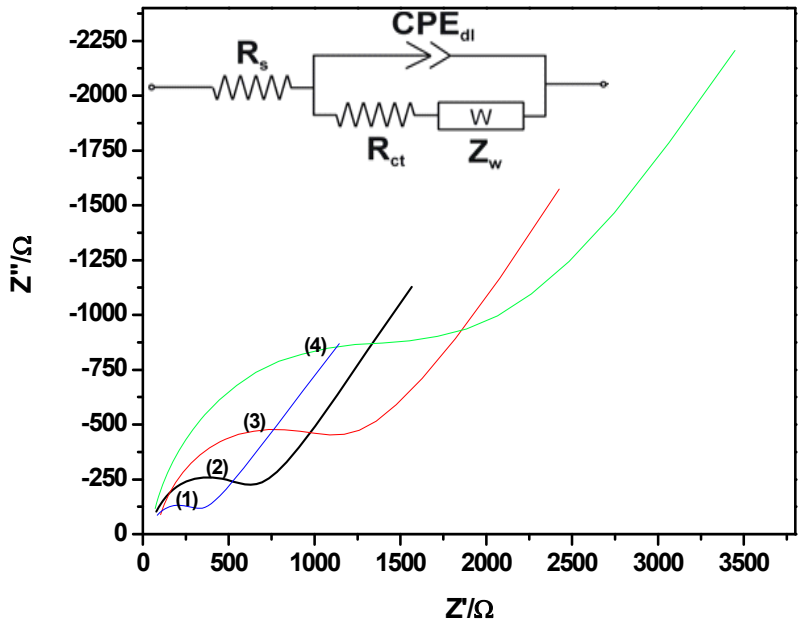

Figure 15A. Nyquist plot of the Faradaic impedance measurements after each incubation steps. Measurements were performed in 2.5 mM $Fe(CN)_6^{3-/4-}$, within a frequency range from 100 mHz to 100 kHz. **(1)** The GNP|OvoxPpy||GCE. **(2)** Electrode after transglutaminase immobilization. **(3)** Electrode after blocking with BSA. **(4)** Immunosensor after incubation with an anti-transglutaminase antibody solution.

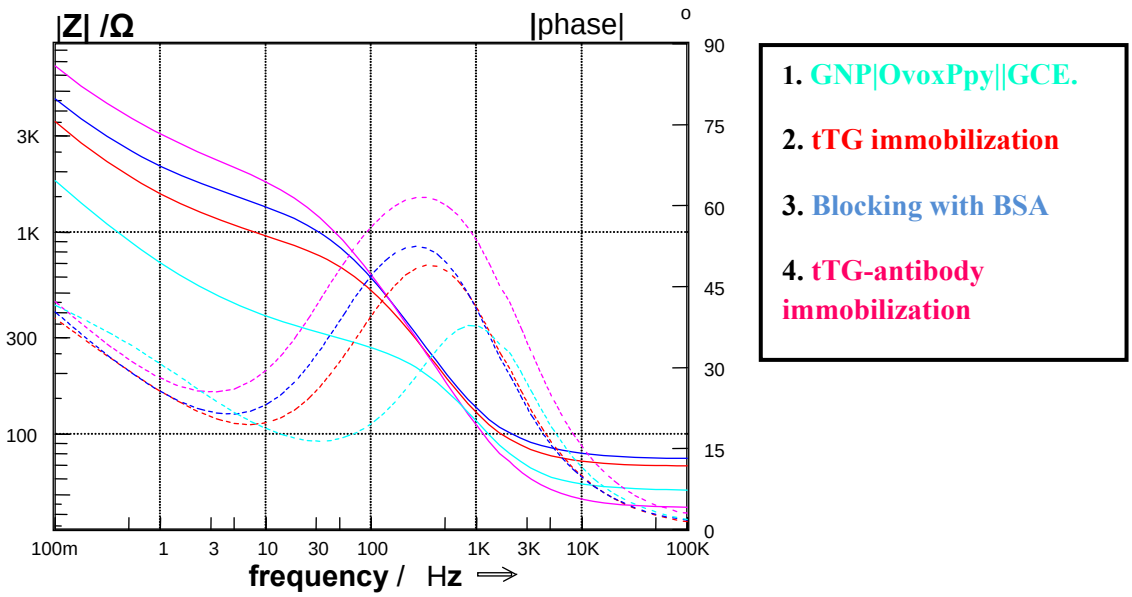

Figure 15B. Bode Plot of data points measured for the GCE after each incubation steps. Measurements were performed in 2.5 mM Fe $(CN)_6^{3-/4-}$ redox probe, within a frequency range from 100 mHz to 100 kHz.

Table 2. Characterization of the different sensor phases in Fe $(CN)_6^{3-/4-}$ redox probe.

	GNP|OvoxPpy||GCE	tTG-antigen	BSA blocking	Anti-tTG_ antibody (1:1000 concentration)
R_{sol}	45.65	45.67	45.71	45.74
R_{ct}(KΩ)	0.271	0.858	1.509	1.652
C_{dl}(μF)	1.694	1.672	1.646	1.602
Z_w	1.872	2.096	2.834	3.084
f_ϕ (Hz)	233.9	265.8	333.9	335.8

Table 3. EIS fitted data for kinetic index of the immunosensor with different antibody concentrations

	1:200	1:500	1:1000	1:2000	1:3000	1:4000
R_{sol}	49.97	49.90	43.66	42.84	42.11	45.65
R_{ct} (KΩ)	2.012	1.679	1.587	1.458	1.337	1.125
C_{dl} (µF)	1.686	1.647	1.603	1.516	1.644	1.486
Z_w (KDW)	6.102	6.616	4.854	5.884	4.531	4.147
f_ϕ (Hz)	211.6	265.8	265.8	285.8	313.9	335.8
τ_1 (s rad^{-1})	3.83×10^{-4}	3.04×10^{-4}	3.05×10^{-4}	2.83×10^{-4}	2.58×10^{-4}	2.39×10^{-4}

5.4 Sensor with different antibody concentrations

The practical application of the GNP|OvoxPpy||GCE with immobilized transglutaminase as immunosensor was demonstrated by establishing a calibration graph with known antibody concentrations. The Fig. 16A shows the effect of dilution on the ΔR_{ct} during the interaction of the immunosensor with standard solutions of anti-transglutaminase antibodies. In this case the electrode consisted of BSA |tTG| GNP|OvoxPpy modified glassy carbon electrode, and was used as the sensing basis for electrochemical impedance analysis of anti-tTG antibody binding to tTG antigen. It can be seen that R_{ct} gradually increased along with the concentration, as a result of more antigen binding to the antibody. The calibration graph resulting from the R_{ct} values determined for different dilutions of a standard antibody solution

(1:4000-1:200) is shown in the Fig 16B. The calibration graph of the immunosensor had a linear fit with correlation value of 0.98 resulting from the ΔR_{ct} values.

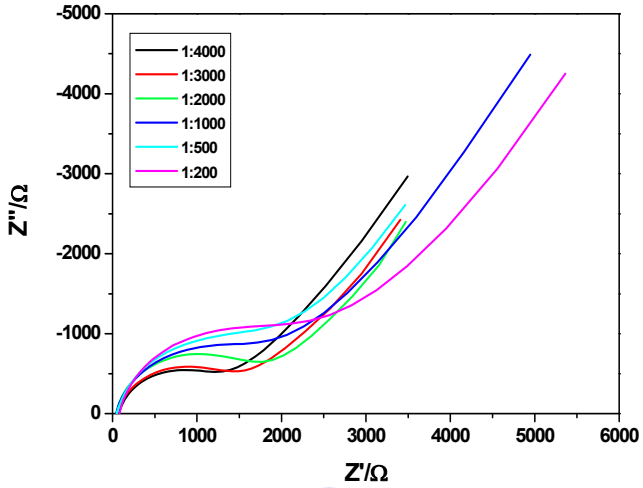

Figure 16A. Nyquist plot of the immunosensor with different anti-transglutaminase antibody concentrations. Measured in 2.5 mM Fe $(CN)_6^{3-/4-}$, within a frequency range of 100 mHz to 100 kHz.

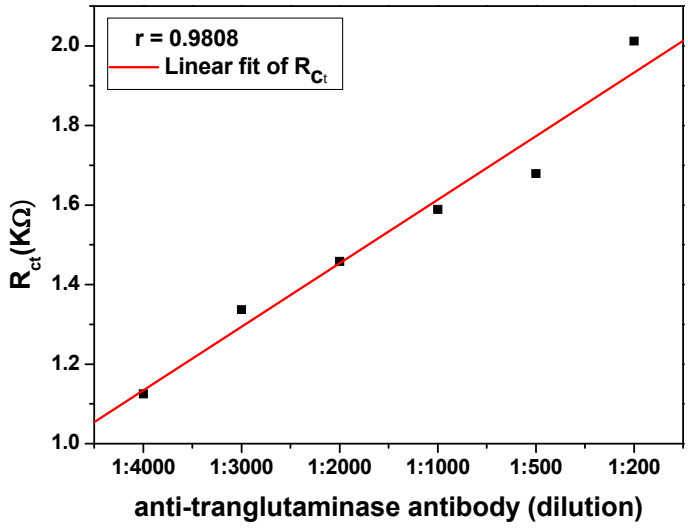

Figure 16B. Calibration graph describing the relationship between the charge transfer resistance ΔR_{ct} and different dilutions of the anti-transglutaminase solutions.

In Table 4 the values of the elements of the Randles circuit derived from a measurement over the whole frequency range are compared to the values evaluated from the measurements at the two selected frequencies. From these two selected measurements, calibration graphs were plotted to establish the deviation from the R_{ct} value. Figure 17 shows the correlation values of 0.99 and 0.98 obtained from the two-point measurement, and deviation from the R_{ct} value of only 1% can be elucidated. This indicates that the fitting of impedance values obtained at 890.3 MHz and 10.3 Hz guarantees a reliable analysis of the immunosensor.

Table 4. Results of the fitting procedure using impedance values measurement over the whole frequency range and from two selected frequencies from, performed in 2.5 mM Fe $(CN)_6^{3-/4-}$.

Dilution	**890.3 mHz**	**10.03 Hz**	**R_{ct}**
1: 200	3.947	2.190	2.012
1: 500	3.701	1.980	1.679
1: 1000	3.163	1.774	1.589
1: 2000	2.542	1.677	1.458
1: 3000	2.205	1.399	1.337
1: 4000	2.194	1.335	1.1125

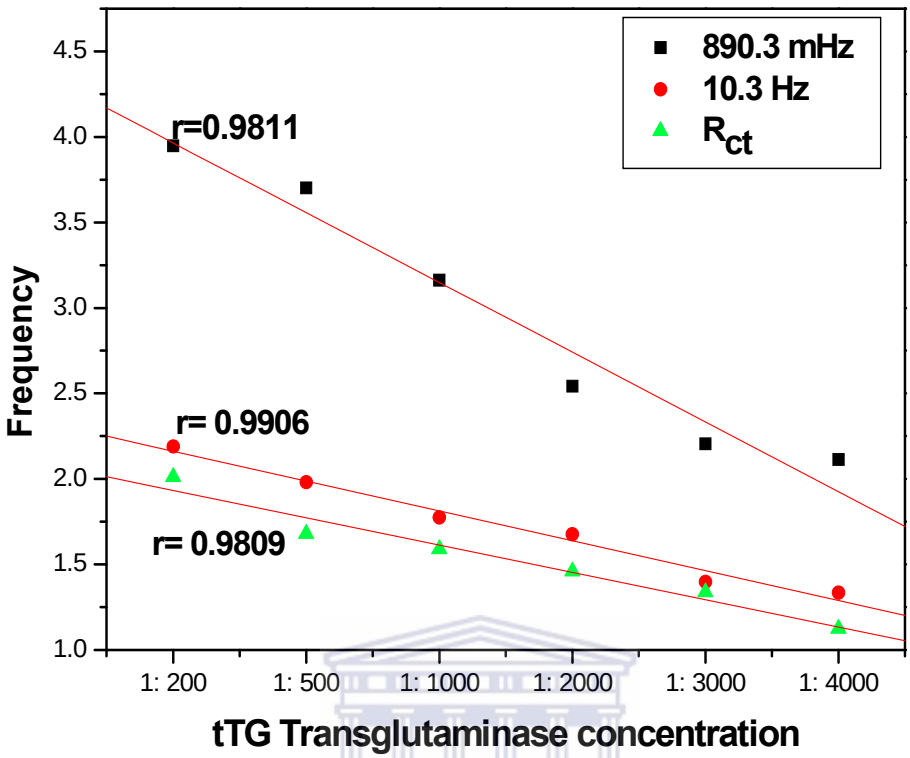

Figure 17. Calibration graph showing the deviation in correlation between the charge transfer resistance and impedance values obtained at 890.3 mHz and 10.3 Hz.

5.6 Storage stability of the immunosensor

The stability of the immunosensor was also investigated. The impedance of the modified electrode gradually decreased after storage, due to the deactivation of the antigen as it is considered to be unstable when stored. From Fig 18B, it was established that the R_{ct} response of the sensor decreased about 7.5% after storage at 4 ºC under dry conditions for 5 days after incubation with 100 µL anti-tTG solution (1:200), compared to the initial values obtained from the same electrode. The good stability of the immunosensor may be ascribed to the selective behavior of the GNP|OvoxPpy film providing an efficient barrier to exclude interferents and prevented the leaking of tTG antigen from the electrode surface by strong binding interaction of the antigen to the platform.

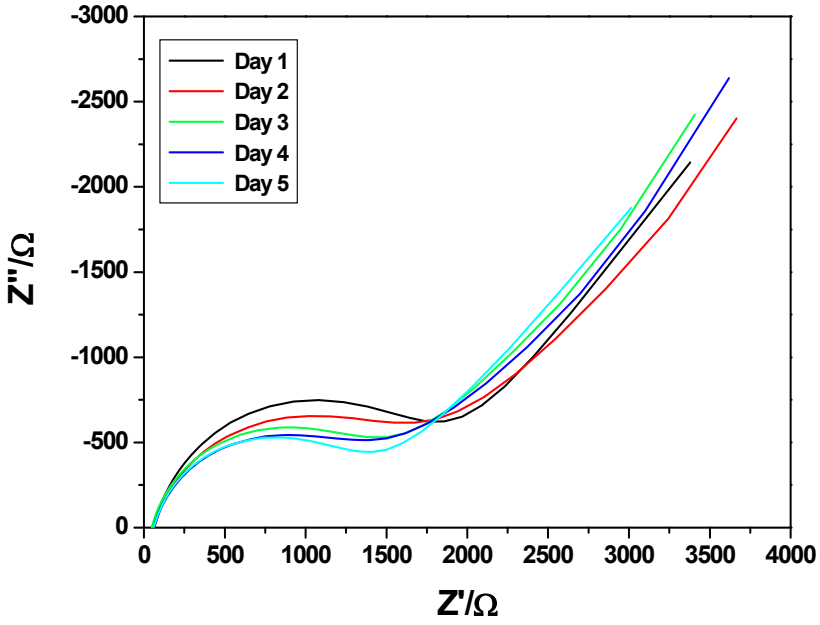

Figure 18A. Nyquist plot showing the stability of the immunosensor

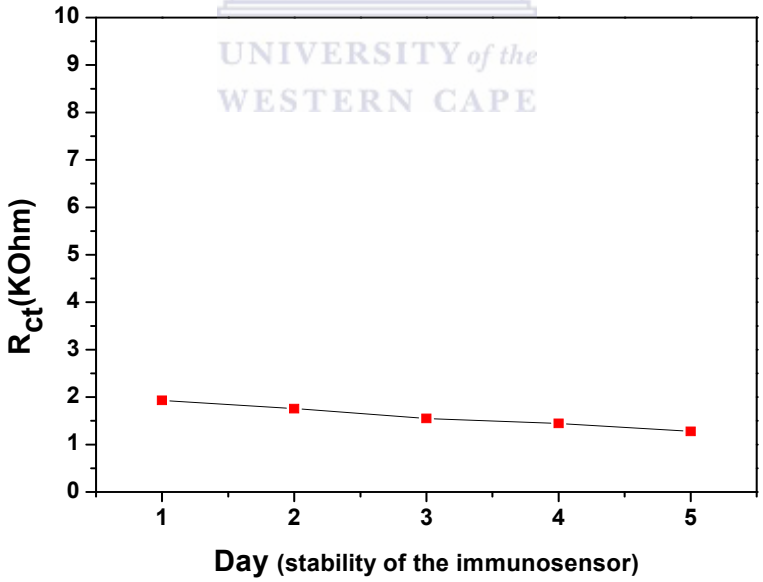

Figure 18B. Linear plot showing the Change in R_{ct} over a period of 5 days.

5.7 Sensor control experiments

Different controls were performed to substantiate the antigen antibody biorecognition and the results are shown in Figures 19, 20 and 21. To achieve this task, the study was done in the presence and absence of antigen and antibody, respectively. As shown in Fig 19, no observable change in R_{ct} was found when the antibody was omitted and only buffer solution was incubated (blank). Comparing with Fig 20, it is observed that in the absence of tTG antigen no bio-recognition event occurs as result there is no observable change in impedance. This can be explained by the fact that tTG is the specific protein that is identified by the anti-tTG antibody and upon binding provide an increase in impedance. Compared with the nanocomposite modified GCE, it is clear that nonspecific proteins are adsorbed on the GCE transducer, increasing the impedimetric signal (Fig 21). Evaluating the behavior of assay procedure shown in Fig 17 and 18, it is clear that the adsorption of tTG on the modified GCE prevents nonspecific adsorption and act as specific capture antigen for the detection of specific antibody present in serum samples.

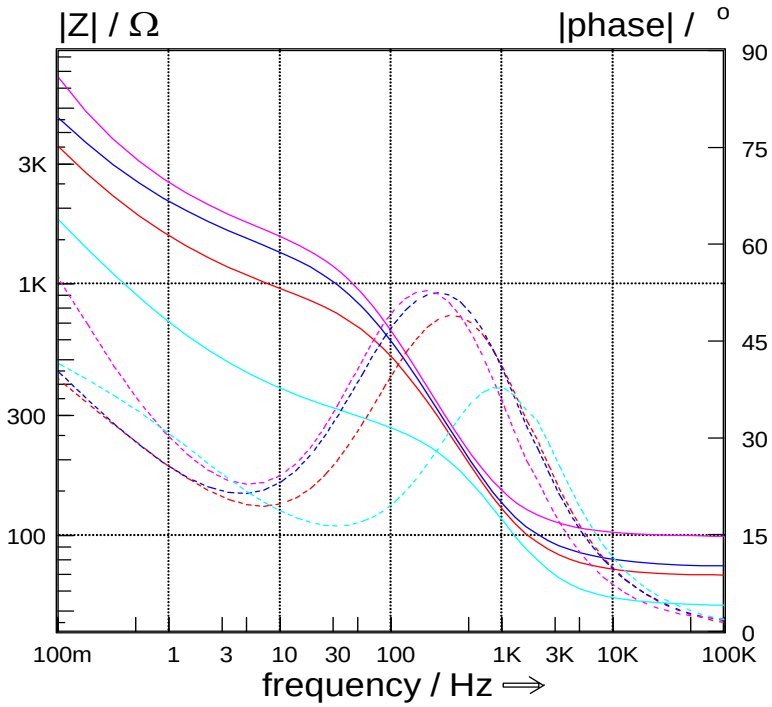

Figure 19 Bode Plot of data points measured for the Au|OvoxPpy||GCE, tTG antigen immobilization , BSA Blocking and PBS (Blank) incubation consecutively.

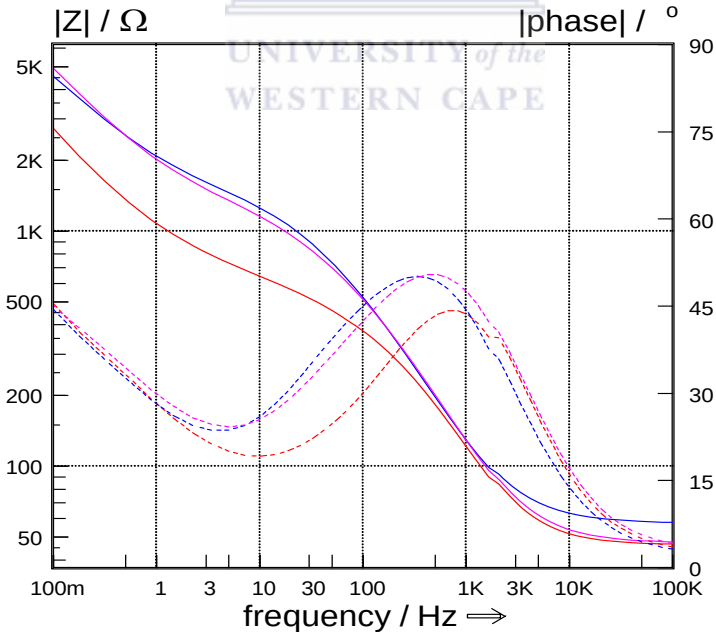

Figure 20 Bode Plot of data points measured for the Au|OvoxPpy||GCE, BSA Blocking and tTG antibody immobilization.

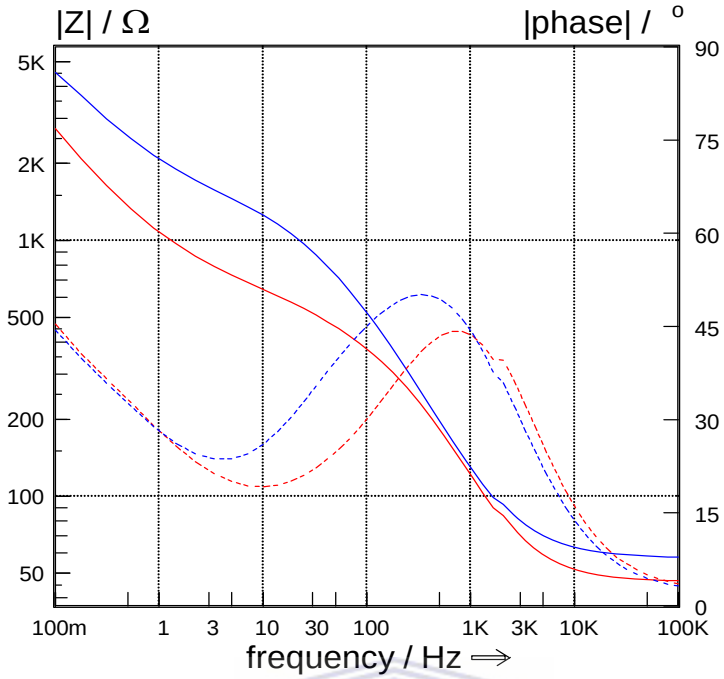

Figure 21 Bode Plot of data points measured for the GNP|OvoxPpy||GCE , BSA Blocking .

Table 5. Results of the fitting procedure for control experiments performed. Measurements were performed in 2.5 mM Fe $(CN)_6^{3-/4-}$ redox probe, within a frequency range from 100 mHz to 100 kHz.

Control	Rct (Ohm)	Cd (µF)	Z_W(KDW)
PBS||Platform	336.2	1.602	4.78
BSA||Platform	0.1070	1.578	3.439
PBS||BSA||Platform	983.6	1.465	3.601
anti-tTG|| Platform	986.2	1.519	4.383
anti-tTG||tTG|| Platform	0.1377	1.346	4.828
anti-tTG||BSA|| tTG|| Platform	0.1721	1.282	5.195
PBS||BSA|| tTG|| Platform	0.1091	1.733	4.691

CHAPTER 6

6.0 CONCLUSIONS AND RECOMMENDATIONS

6.1 Conclusions

In this study the synergic effect of OvoxPpy with Au nano-particles in immunosensor fabrication are reported. The OvoxPpy was shown to be successful as template for Au nanoparticles deposition onto which transglutaminase was immobilized by electrostatic absorption. Transglutaminase is the specific protein that is identified by the anti-tTG antibody, which allows the diagnosis of CD. The electrodeposition technique for the preparation of electroactive polypyrrole modified glassy carbon nanoelectrode was successfully carried out from aqueous solution. The electrodeposition chemistry is simple and thus eliminates complex immobilization chemistries. Due to the synergic effect of OvoxPpy and Au nano-particles, the GNP|OvoxPpy||GCE displayed good stability and selectivity with respect to its protein bind efficiency. The electrochemically synthesized GNP|OvoxPpy on GCE was shown to be an attractive platform for immunosensor fabrication through the study of electrode surface morphology, cyclic voltammetry and immunosensor performance. This approach can be miniaturized and commercialized on screen printed carbon electrodes. The nanoelectrode was redox active, conducting and catalyzed the redox process of $[Fe(CN)_6]^{3-/4-}$.

Results have shown that the high stability of the gold nanoparticles adsorbed onto the OvoxPpy film provides enhanced antigen immobilization and keep efficient activity retention. Exposing the developed immunosensor to subsequent incubation steps, which included blocking of unspecific and residual binding sites with bovine serum albumin and incubating the immunosensor with standard solutions of anti-transglutaminase antibodies

(from goat), respectively, resulted in an increase of the interfacial impedance of the sensor electrode. This increase was measured by electrochemical impedance spectroscopy. The electrochemical response of a redox probe system Fe $(CN)_6^{3-/4-}$ was effective as a signal for the presence of agglutination reactions on the electrode surface. By fitting the impedance spectra to a Randles equivalent circuit containing a constant phase element (CPE), the charge transfer resistance (R_{ct}) was found to correlate with the antibody concentration and was used as the sensor parameter. A calibration graph with correlation value of 0.98 was established for the immunosensor with different anti-transglutaminase antibody concentrations. Furthermore, the recording of impedance spectra of the immunosensor can be simplified by the measurement and analysis of only two selected frequencies (890.3 mHz and 10.03 Hz) without loss of reliability.

6.2 Recommendations

The availability of the OvoxPpy film and further design of its surface chemistry in combination with metal nanoparticles could be an interesting stratagem for high efficient and high selective electrochemical sensor designs. The proposed methodology shows great potential to be further developed for practical clinical detection of anti-tTG antibody in human serum.

REFERENCES

1. Adeloju SB and Moline AN, Fabrication of ultra-thin polypyrrole–glucose oxidase film from supporting electrolyte-free monomer solution for potentiometric biosensing of glucose. *Biosens Bioelectron* **16**:133-139 (2001).
2. Razola SS, Ruiz BL, Diez NM, Mark HB and Kauffmann JM, Hydrogen peroxide sensitive amperometric biosensor based on horseradish peroxidase entrapped in a polypyrrole electrode. *Biosens Bioelectron* **17**:921-928 (2002).
3. Kum MC, Joshi KA, Chen W, Myung NV and Mulchandani A, Biomolecules-carbon nanotubes doped conducting polymer nanocomposites and their sensor application. *Talanta* **74**:370-375 (2007).
4. Wu L, McIntosh M, Zhang XJ and Ju HX, Amperometric sensor for ethanol based on one-step electropolymerization of thionine-carbon nanofiber nanocomposite containing alcohol oxidase. *Talanta* **74**:387-392 (2007).
5. Wang JJ, Myung NV, Yun M and Monbouquette HG, *J ElectroanalChem* **575**:139-146 (2005).
6. Chu X, Duan DX, Shen GL and Yu RQ, Amperometric glucose biosensor based on electrodeposition of platinum nanoparticles onto covalently immobilized carbon nanotube electrode. *Talanta* **71**:2040-2047 (2007).
7. Jing L and Xiang-Qin L, Electrodeposition of gold nanoclusters on overoxidized polypyrrole film modified glassy carbon electrode and its application for the simultaneous determination of epinephrine and uric acid under coexistence of ascorbic acid. *Anal Chim Acta* **596**:222-230 (2007).
8. Viticoli M, Curulli A, Cusma A, Kaciulis S, Nunziante S, Pandolfi L, Valentini F and Padeletti G, Third-generation biosensors based on TiO2 nanostructured films. *Mater Sci Eng* **26**:947-951 (2006).
9. Du D, Ding JW, Cai J and Zhang AD, Amperometric detection of triazophos pesticide using acetylcholinesterase biosensor based on multiwall carbon nanotube–chitosan matrix. *Sens Actuators B: Chem* **127**:317-322 (2007).
10. Liu S, Wollenberger U, Katterle M and Scheller FW, *Sens Actuators B:Chem* **113**:623-629 (2006).

11. Mala Ekanayake EMI, Preethichandra DMG and Kaneto K, Polypyrrole nanotube array sensor for enhanced adsorption of glucose oxidase in glucose biosensors. *Biosens Bioelectron* **23**:107-113 (2007).
12. Wang M, Wang L, Wang G, Ji X, Bai Y, Li T, Gong S and Li J, Application of impedance spectroscopy for monitoring colloid Au-enhanced antibody immobilization and antibody-antigen reactions. *Biosens Bioelectron* **19**:575-582 (2004).
13. Strike DJ, Rooij NFD, Koudelkahep M, Ulmann M and Augustynski J, Electrocatalytic oxidation of methanol on platinum microparticles in polypyrrole. *J Appl Electrochem* **22**:922-926 (1992).
14. Rau JR, Chen SC and Sun HW, Characterization of a polypyrrole microsensor for nitrate and nitrite ions *Electrochim Acta* **39**:2773-2779 (1994).
15. Lisdat F, Ge B, Krause B, Ehrlich A, Bienert H and Scheller FW, Nucleic acid-promoted electron transfer to cytochrome c. *Electroanalysis* **13**:1225-1230 (2001).
16. Rubinstein I, Physical Electrochemistry, Marcel Dekker Inc., New York (1995).
17. Reif S and Lerner A, Tissue transglutaminase-the key player in celiac disease: a review. *Elsevier*:40-45 (2004).
18. Spinks GM, Domins AJ, Wallace GG and Tallman DE, Electroactive conducting polymers for corrosion control: Part 2. Ferrous metals *Solid state electrochem* **6**:85-100 (2002).
19. Boinowitz T and Beck F, A quantitative discrimination between anion insertion- and surface redox-reactions at graphite with the rotating ring/disk-electrode. *ElectroanalChem* **461** (1999).
20. Skotheim TAE (ed.) *Handbook of Conducting Polymers* Marcel Dekker, New York (1986).
21. Inzelt G, Pineri M, Schultz JW and M.A V, Simultaneous chronoamperometric and quartz crystal microbalance studies of redox transformations of polyaniline films. *Electrochim Acta* **45** (2000).
22. Amine A, Mohammadi H, Bourais I and Pallesschi G, Enzyme inhibition-based biosensors for food safety and environmental monitoring. *Biosens Bioelectron* **21** (2006).

23. Sotiropoulou S and Chaniotakis NA, Lowering the detection limit of the acetylcholinesterase biosensor using a nanoporous carbon matrix *AnalChimActa* **530**:199-204 (2005).
24. Yadavalli VK, Koh WG, Lazur GJ and Pishko MV, Microfabricated protein-containing poly(ethylene glycol) hydrogel arrays for biosensing. *SensActuators B Chem* **97**:290-297 (2004).
25. Solna R, hristonson E, Winther-Nielson M, Carlsson C, Emneus J, Ruzgas T and Skliadal P, Amperometric screen-printed biosensor arrays with co-immobilised oxidoreductases and cholinesterases. *Anal Chim Acta* **528** (2005).
26. Lin Y, Lu F and Wang J, Disposable Carbon Nanotube Modified Screen-Printed Biosensor for Amperometric Detection of Organophosphorus Pesticides and Nerve Agents *Electroanalysis* **16**:145-149 (2004).
27. Gill I and Ballestosteros A, *Trends Biotechnol* **15** (2000).
28. Migdalshi J, Blaz T and Lewenstam A, *Anal Chim Acta* **322** (1996).
29. Gao Z, Zi M and Chen B, The influence of overoxidation treatment on the permeability of polypyrrole films. *JElectroanal Chem* **373** (1994).
30. Beck F, Braun P, Oberst M and Bunsenges B, *Phys Chem* **91** (1987).
31. (Ed). MAH (ed.) *Colloical Gold-Principles*. Academic Press, San Diego (1989).
32. Suelter CH and Kricka L (eds.), *Colloical Gold-Principles, Methods and Applications*. Academic Press, San Diego (1992).
33. Eggins BR, Chemical sensors & biosensors, John Wiley & Sons Ltd, UK, p 78 (2003).
34. Wieser H and Baillieres C, The precipitating factor in coeliac disease. *Bailliere's Clinical Gastroenterology* **9**:191-207 (1995).
35. Shan L, Molgerg O, Parrot I, Hausch F, Filiz F, Gray GM, Sollid LM and Khosla C, Structural basis for gluten intolerance in Celiac Sprue. *Science* **297**:2275- 2279 (2002).
36. Sollid LM, Coeliac disease: Dissecting a complex inflammatory disorder *Nat Rev Immunol* **2**:647-655 (2002).
37. Lee A and Newman JM, Celiac diet: Its impact on quality of life. *J Am Diet Assoc* **103**:1533- 1535 (2003).

38. Dieterich W, Ehnis T and Bauer M, Identification of tissue transglutaminase as the autoantigen of celiac disease. *Nat Med* **3**:797-801 (1997).
39. Rostom A, Murray J and Kagnoff M, American Gastroenterological Association (AGA) Institute technical review on the diagnosis and management of celiac disease. *Gastroenterology* **131**:1981-2002 (2006).
40. Lenhardt A, Plebani A and Marchetti F, Role of human-tissue transglutaminase IgG and anti-gliadin IgG antibodies in the diagnosis of coeliac disease in patients with selective immunoglobulin A deficiency. *Dig Liver Dis* **36**:730-734 (2004).
41. Dieterich W, Ehnis T, Bauer M, Donner P, Volta U, Riechen E and Schuppan D, Identification of tissue transglutaminase as the autoantigen of coeliac disease. *Nature Med* **3**:797-801 (1997).
42. Fesus L and Piacentini M, Transglutaminase 2: an enigmatic enzyme with diverse functions. *Trends Biochem Sci* **27**:534-539 (2002).
43. Nirova K and Bazovoski S, The electrochemistry of antibody-modified conducting polymer electrodes. *Synthetic Metals* **76** (1996).
44. Kim J, Grate JW and Wang P, Nanostructures for enzyme stabilization. *Chemical Engineering Science* **61** (2006).
45. Balkenhohl T, Screen-printed electrodes as impedimetric immunosensors for the detection of anti-transglutaminase antibodies in human sera. *Analytical Chimica Acta* **597**:50-57 (2007).
46. Karube I and Nomura Y, Enzyme sensors for environmental analysis. *J Mol Catal B: Enzym* **10**:177-181 (2000).
47. Hill HAO and Sanghera GS (eds.), *Mediated amperometric enzyme electrodes*. Biosensors; A Practical Approach (ed Cass, A.E.G.), Oxford University (1990).
48. Cui X, Pei R, Wang Z, Yang F, Ma Y, Dong S and Yang X, Electrochemical Biosensors based on layer-by-layer Assemblies. *Biosens Bioelectron* **18** (2003).
49. Oswald B, Lehman F, Simon L, Terpetschnig E and Wolfbeis OS, Red Laser-Induced Fluorescence Energy Transfer in an Immunosystem. *Anal Biochem* **280** (2000).
50. Coulet PR (ed.) *What is a biosensor?* Blum, L. J. and Coulet, P.R. (Ed), New York (1991).
51. Harlow E and Lane D, Antibodies- A Laboratory Manual, Cold Spring Harbor Laboratory, New York (1988).

52. Killard AJ, Deasy B, O'Kennedy R and Smyth MR, *Trends Anal Chem* **14** (1996).
53. Blum LJ, Bio-and Chemi-Luminescent Sensors., World Scientific Publishing, Singapore, pp 5-20 (1997).
54. Barker SA (ed.) *Immobilization of the biological component of biosensors*. Oxford University Press, Oxford.
55. Srere PA and Uyeda K, *Method in Enzymology* (1976).
56. Gemeiner P (ed.) *Enzyme engineering* New York (1992).
57. Broum GB, The Application of Coenzyme-Dependent Enzymes in Biotechnology [and Discussion]. *Methods in Enzymology* **300** (1976).
58. Ren X and Pickup PG, *J Phys Chem* **97** (1993).
59. Xu H, Masila M, Yan F and Sadik OA, Multiarray sensors for pesticides and toxic metals, Proc. SPIE-Int. Soc. Opt., England, p 437 (1999).
60. Sargent T, Loi S, Gal OA and Sadik J, *Electroanal Chem* **470**:144-156 (1990).
61. Heller A, Electrical wiring of redox and enzymes. *Acc Chem Res* **23**:128-134 (1990).
62. Wallace JL, Vergnolle N, Muscara MN, Asfaha S, Chapman K, McKnight W, Del Soldato P, Morelli A and Fiorucci S, Enhanced anti-inflammatory effects of a nitric oxide-releasing derivative of mesalamine in rats. *Gastroenterology* **117** (1999).
63. Bartlett PW and Whitaker RG, Electrochemical immobilisation of enzymes. Part II. Glucose oxidase immobilised in poly-N-methylpyrrole. *J Electroanal Chem* **224** (1987).
64. Detaxis Du Poet P and Miyamoto S, Enzyme Modified Electrodes in Amperometric Biosensors. *Anal Chimica Acta* **235** (1990).
65. Murray RW, Ewing AG and Durst R, A, Chemically modified electrodes. Molecular design for electroanalysis. *Anal Chem* **59**:379A-390A (1987).
66. Sadik O and Wallace G, Pulsed amperometric detection of proteins using antibody containing conducting polymers. *Anal Chim Acta* **279**:209-212 (1993).
67. Ren X and Pickup PG, An impedance study of electron transport and electron transfer in composite polypyrrole + polystyrenesulphonate films. *J Phys Chem* **97** (1993).
68. Barbero G, Alexe-lonescu AL and Lelidis I, Significance of small voltage in impedance spectroscopy measurements on electrolytic cell. *J Appl Phys* **89** (2005).
69. Bard AJ and Faulkner LR (eds.), *Electrochemical Methods:* Fundamentals and applications Wiley, New York (2001).

70. Berggren C, Bjamason B and Johansson G, Instrumentation for direct capacitive biosensors. *Instrum Sci Technol* **27**:131-137 (1999).
71. Kahlert H, Electroanalytical methods: Guide to Experiments and Applications, in *Springer*, Scholz, F, New York, pp 261- 278 (2002).
72. Macdonald DD, Reflections on the history of electrochemical impedance spectroscopy. *Electrochim Acta* **51**:1376-1388 (2006).
73. Pajkossy T, Impedance of rough capacitive electrodes. *J Electroanal Chem* **364**:111-125 (1994).
74. Kerner Z and Pajkossy T, On the origin of capacitance dispersion of rough electrodes *Electrochim Acta* **46**:207-211 (2000).
75. Brett MAC and Brett AMO (eds.), *Electrochemistry Principles, Methods and Applications*. Oxford University Press, New York (1999).
76. Zhou Y, Itoh H, Uemura T, Naka K and Chujo Y, Preparation of pi-conjugated polymer-protected gold nanoparticles in stable colloidal form. *Chemical Communication* (2007).
77. Boinowitz T and Beck F, *ElectroanalChem* **461** (1999).
78. Geetha S, Chepuri RK, Rao M and Vijayan DC, Biosensing and drug delivery by polypyrrole. *Analytical Chimica Acta* (2005).
79. Aminur R, Pankaj K, Deog-Su P and Yoon-Bo S, Electrochemical Sensors Based on Organic Conjugated Polymers. *Sensors* **8**:118-141 (2008).
80. Pei RJ, Cheng ZL, Wang EK and Yang XR, Electrostatic layer-by-layer assembly of polycation and DNA multilayer films by real-time surface plasmon resonance technique *Chinese Journal of Chemistry* **19**:433-435 (2001).
81. Orazem ME and Tribollet B (eds.), *Electrochemical Impedance Spectroscopy*. Hoboken, New Jersey (2008).